International Journal of Pharmaceutics 628 (2022) 122323

Contents lists available at ScienceDirect

International Journal of Pharmaceutics

journal homepage: www.elsevier.com/locate/ijpharm

Development of chloramphenicol whey protein-based microparticles incorporated into thermoresponsive in situ hydrogels for improved wound healing treatment

Ardiyah Nurul Fitri Marzaman [a], Sartini [a], Mukarram Mudjahid [a], Tri Puspita Roska [a], Anwar Sam [b], Andi Dian Permana [a,*]

[a] Department of Pharmaceutical Science and Technology, Faculty of Pharmacy, Hasanuddin University, Indonesia
[b] Department of Pharmacy, Faculty of Pharmacy, Hasanuddin University, Indonesia

ARTICLE INFO

Keywords:
Antimicrobial
Skin infection
Chloramphenicol
Microparticle
Thermoresponsive-gel, whey-protein

ABSTRACT

This study focused on the incorporation of chloramphenicol (CAP) into whey protein (WPI) (CAP-MPs) and was further formulated into a thermoresponsive in situ gel for wound healing treatment. CAP microparticles were produced by two steps emulsification process. The modification of the mixing time and speed, as well as the variation of WPI and CAP concentration, resulted in various particle sizes (0.95 ± 0.07 to 8.94 ± 0.32 μm). The optimum formulation was achieved using 15 % WPI in water, and 2 mL CAP in propylene glycol with a total amount in the mixture was 100 mg, and 5 % oil phase, with homogenization time and speed at 15 min and 7500 rpm, respectively. The characterization of CAP-MP's showed PDI values at 0.110 ± 0.007, drug entrapment efficiency at 70.64 ± 1.12 %, and drug loading at 8.80 ± 0.12 %. SEM analysis of CAP-MPs showed spherical, uniform particles dispersed across the surface of the emulsion droplets. FTIR analysis showed strong development of hydrogen bonds proving the encapsulation was effective. Pluronic® F127, Pluronic® F68, and hydroxypropyl methylcellulose (HPMC) were used for the thermoresponsive hydrogel formulation with desired properties. The gel formulation could provide liquid form at room temperature (25 °C) and form a gel at 31 °C. This optimum formula was able to increase the bioadhesivity (28160.92 ± 3902.09 dyne/cm^2) as well as the percentage of gels skin occlusivity after 24 h (32.82 ± 0.004), and to be considered, it did not show hemolytic activities. In an ex vivo antibacterial activity, this combination approach showed a 99.95 % reduction in the - Staphylococcus aureus (SA) population.

1. Introduction

Dermatological, subcutaneous, and epidermal infections were all examples of skin and soft tissue infections (SSTI). Severe complications, such as sepsis, endocarditis, and osteomyelitis, might occur as a result of these skin diseases (Dahlman et al., ujyh). An increasing number of skin infections have been linked to an increased risk of death, with an associated case-fatality ratio of 20.3 % and an annual mortality rate of 3.4 per 100,000 people (Hasan et al., 2019). Polymicrobial skin infections, which could be predictable, and biofilm production have also been highlighted in past literature as the main causes of the failures of medication (Clinton and Carter, 2015). Nowadays, Fighting polymicrobial diseases necessitated ongoing research into prevention and treatment in a more advanced approach (Sartini et al., 2021).

Known as a broad-spectrum antibiotic, chloramphenicol acts by binding reversibly to the 50S subunit of the 70S ribosome, which inhibits the synthesis of bacterial ribosomes from soluble RNA, therefore interfering with bacterial peptide bond production (A. Y. Shen et al., 2018). Chloramphenicol, when used orally, could cause bone marrow poisoning and aplastic anemia, both of which are irreversible (Kalita et al., 2015). To treat bacterial conjunctivitis, chloramphenicol ointment has been used. Due to its hydrophobic chemical composition, chloramphenicol was not used for the topical treatment of skin infections and has not been studied extensively for specific adverse effects if the drug was delivered topically (A. Y. Shen et al., 2018). To overcome the several disadvantages of chloramphenicol, it was proposed to be created to use on the skin, to decrease the systemic exposure and targeted the desired infected site. Drug delivery systems in the form of

* Corresponding author.
E-mail address: andi.dian.permana@farmasi.unhas.ac.id (A.D. Permana).

https://doi.org/10.1016/j.ijpharm.2022.122323
Received 14 September 2022; Received in revised form 14 October 2022; Accepted 15 October 2022
Available online 21 October 2022

creams, ointments, and gels could be applied to the skin in a variety of ways, including the appendageal route and the transepidermal route (Cheung and Das, 2016). However, no research has been done to see if it may also be used to prevent or treat wound or burn infections. The thickening of the human skin creates an impenetrable barrier that prevents the transdermal transport of hydrophobic medicines (Kalita et al., 2015); hence, a skin barrier-penetrating drug delivery device must be developed. Not only does the skin barrier become the challenge of drug development, but it also takes a long time to treat infection due to the low drug concentrations in certain infected tissues (Permana et al., 2020a,b).

Encapsulation into microparticles or nanoparticle delivery methods is now being studied to improve therapeutically available antibiotics' potency against biofilms (Ferreira et al., 2015). With a longer medication retention rate in skin tissue, microparticles were favored compared to nanoparticles for local infection targets. This is because the infected tissue produces more of certain bacterial enzymes, has a lower pH, and has a variety of surface charges. The microparticle system can be modified to slowly release the medicine where it is needed, as a solution of the low concentration of hydrophobic drugs was localized in the infection site (Mir et al., 2019).

Whey protein (WP), a natural polymer, is employed in the pharmaceutical industry because it may generate foaming, emulsions, and gels (Bourgeois et al., 2019). Combrinck et al. have successfully used WP as an encapsulation agent which showed to be the most effective for protein delivery via the cutaneous and transdermal routes of transportation (Combrinck et al., 2014). Whey protein is known to undergo a dimensional rearrangement and the emergence of active protein sites as a result of heat treatment. Disulfide bonds, hydrogen bonds, and van der Waals interactions can develop as a result of this aggregation of proteins (Picone et al., 2011).

To distribute microparticles in the dermal system, the preparation was created in the form of a thermoresponsive gel that will form a gel in situ due to the changes in temperature so that it could change to a gel and release the medication in a sustainable or controlled manner (Majeed and Khan, 2019). In preparations for the treatment of burns, topical administration of anticancer agents, continuous drug delivery, and transdermal application, the polymer Poloxamer 407 or formerly known as Pluronic® F127 can be used; it has undergone extensive research. This polymer can be used in gels, microemulsions, nanoparticles, and solid polymer formulation (Wang et al., 2017). The gelling agent was amphiphilic and had thermogelling properties making it an ideal drug carrier for a wide range of small and big molecules, including proteins (Wang et al., 2017). In order to limit toxicity, dermal delivery devices have been developed, which could target specific locations of infections.

Furthermore, an ex vivo dermatokinetic study with a rat's skin infection model was conducted to evaluate the efficiency of this method. The results of this study showed that drug microparticle delivery devices could be applied to the skin. Microparticles incorporated in Pluronic® F127 and Pluronic® F68 polymers, as explained above, have been used to develop new antibacterial medications that can be more successful at stopping the growth of Staphylococcus aureus. The gels' bioadhesivity in the skin is enhanced by the addition of hydroxypropyl methylcellulose (HPMC). In vitro and ex vivo efficacy tests, as well as further evaluations and characterizations, were performed.

2. Materials and method

2.1. Materials

Chloramphenicol (CAP) was purchased from Merck (Darmstadt, Germany). Glanbia Nutritionals, Inc, Fitchburg, USA. generously supplied the whey protein isolate (WPI). According to the producer, WPI consists of 80 % protein isolate. Sigma-Aldrich was used to acquire Pluronic F127 and F68 (Singapore) also Tryptone Soy Agar (TSA) and Tryptone Soy Broth (TSB) medium. The analytical quality was maintained with all other reagents. In every step, filtered Milli-Q water was utilized instead.

2.2. Chloramphenicol microparticles (CAP-MP'S) preparation

Using a modified two-step emulsification process, Chloramphenicol (CAP) microparticles were prepared to create heat-induced WPI microparticles (CAP-MPs) (Sağlam et al., 2011). WPI powder was dispersed in Milli-Q water (w/w). The final concentration of the WPI solutions was made at 5 %, 10 %, 15 %, and 20 %. The dispersion was chilled after being agitated overnight to dissolve the WPI. Furthermore, CAP was dissolved in 2 mL propylene glycol (PG) to achieve final concentration at 25, 50, 100, 200, and 400 mg. The WPI solution was progressively blended into SPAN in VCO (5 %) which acts as the oil phase in the emulsion. The overall mixing time was set at 5 to 20 min. The mixing speeds were set to 1250,2500, 5000, and 7500 rpm using a high-speed mixer (Ultra-turrax T 18, IKA, Germany). Further emulsification was achieved by heating the primary emulsion to 80 °C while stirring it with a magnetic stirrer at 500 rpm. The procedure was over when the emulsion formed the translucent phase. In this step, WPI proteins were expected to be crosslinked and produce microparticles with the drug components. The surplus oil from the formulation needed to be removed, so it was centrifuged for 1 h at 8000 rpm. The filtrate, protein microparticles, was rinsed with Milli-Q water and centrifuged to remove any remaining oil. The procedure was done three times before the CAP-MP's were freeze-dried and kept at 4 °C.

2.3. Microparticles (CAP-MP'S) characterization

2.3.1. Determination of particle Size, polydispersityindex (PDI), and zeta potential

Particle size and size distribution were determined using a Mastersizer 2000 size analyzer (Malvern Instruments, Malvern, UK). The zeta potential was determined using a Zetasizer Nano ZS (Malvern Instruments, Malvern, UK).

2.3.2. Calculation of % encapsulation and drug loading efficiency

The CAP-MP's suspension was dissolved and centrifuged at 5000 rpm for 10 min. The supernatant was taken and then analyzed using a UV–vis spectrophotometer according to a derivatization method described by (Alshirifi, et al.) with a visible wavelength. The use of the derivatization method was due to the presence of overlapping peaks between the CAP and WPI when measured at UV wavelength. The spectrophotometric method is based on the condensation reaction between 0.01 M sodium bicarbonate, 100 ppm of CAP stock solution, 0.01 M of 1,2 naphthoquinone-4-sulfonic (1,2 NQS) as a reagent to form an orange-red product. The reducing nitro group in drug components of CAP-MP's into the amino group was achieved by the use of 0.5 mL concentrated HCl and 300 mg zinc powder while being heated and stirred for 5 min in a water bath at 50 °C. The reduced solution was allowed to cool for 15 min before being filtered to 100 mL in a calibrated flask. Furthermore, it was diluted using distilled water. The Orange-red product was measured at 489 nm to determine the amount of CAP encapsulated in the microparticles. The calculation of % encapsulation efficiency (EE) and % drug loading (DL) follows the following equation respectively:

$$\%DL = \frac{\text{Amount of Encapsulated Drug}}{\text{Total Weight}} \text{x } 100\% \quad (1)$$

$$\%EE = \frac{\text{Drug Total} - \text{Drug Free}}{\text{Drug Total}} \text{x } 100\% \quad (2)$$

2.3.3. Scanning electron Microscope.

A scanning electron microscope (SEM) (TM3030 microscope; Hitachi, Krefeld, Germany) was used to examine the sample particles with

the microscope set at 20 kV and a magnification range of 900–1200. The double-sided sticky tape was used to secure the powders to 1 cm in diameter by 1 cm in height SEM stubs before being coated with gold in a vacuum evaporator for examination.

2.3.4. FTIR Study.

Through the use of an FTIR spectrophotometer (Accutrac FT/IR-4100™ Series, Perkin Elmer, USA), we analyzed the components of CAP and CAP in MP's formulation to look for evidence of their interactions. Samples of CAP, CAP-MP's, WPI, and the physical mixture of CAP & WPI (1:1) were run through an FTIR spectrophotometer and scanned between 400 and 400 cm^{-1} in the wavenumber region.

2.3.5. Differential scanning calorimetry (DSC)

Freeze-dried WPI, CAP, CAP:WPI (1:1), and CAP-MP's formulations were all compared for their thermal characteristics. Using an alumina pan and a dynamic nitrogen environment with a flow rate of 100 mL min^{-1}, a heating rate of 10 °C min^{-1}, and a temperature range of 50–550 °C, curves were produced using a TGA50H thermobalance (DSC 2920, TA Instruments, Surrey, UK). The amount of sample used was 5–10 mg.

2.3.6. X-ray diffraction (XRD)

Formulations were powdered, positioned, and covered with glass. Measurements were completed using a Shimadzu X-ray diffractometer (Rigaku Corporation, Kent, England) and Cu-Kα1 radiation with a wavelength of 1.54 Å at 30 kV and 30 mA. Samples were evaluated at angles that range from 4°to 40° in 2 h with an increment of 0.02° (1.2°/min^{-1}) (Botrel et al., 2016).

2.3.7. In vitro drug released studies of CAP-MP's

In vitro drug release of CAP MP's and CAP-only was evaluated using simulated wound fluid which consisted of sodium hydrogen carbonate 0.36 g, sodium chloride 5.84 g, calcium chloride 0.28 g, potassium chloride 30.30 g, and bovine albumin 33.00 g in 1000 mL of deionized water. The simulated wound fluid for each formula was put in two different flasks consisting of 50 mL total volume. The amount of CAP-MP's equivalent to 50 mg of CAP was added into simulated wound fluid. At predetermined time intervals (0.25 h, 0.5 h, 1 h, 2 h, 3 h, 4 h, 5 h, 6 h, 7 h, 8 h, and 24 h), 5 mL of samples taken and replaced with the same volume of new release media. The test was carried out at a temperature of 37 °C and a speed of mixing at 100 rpm. The CAP drug percentages were further examined using a UV–vis spectrophotometer (Shimadzu® FTIR-8400) and following the derivatization procedure in section 2.3.2.

2.3.8. Drug released kinetic using mathematical modelling

A variety of mathematical models were used to estimate the rate of drug release, and the results were presented below (Permana et al., 2019; Permana and Donnelly, 2019)

$$Zeroorderkinetics: C_t = C_0 + k_0 t \quad (3)$$

$$Firstorderkinetics: \ln C_t = \ln C_0 + K_1 t \quad (4)$$

$$HiguchiModel: C_t = k_H \ddot{O} t \quad (5)$$

$$Korsmeyer - Peppas: C_t = k_{kp} t^n \quad (6)$$

$$HixsonCrowell: C_t^{1/3} - C_0^{1/3} = K_{HC}^t \quad (7)$$

where C_t (%) is the percentage of drug released at time t, C_0 is the initial value of C_t, t is the time, n is the diffusion release exponent, K_0, K_1, K_H, K_P, and K_{HC} were the release coefficients corresponding to relevant kinetic models. DD-Solver software was utilized to calculate the model parameters (Zhang et al., 2010).

2.4. Determination of antibacterial activity in vitro

2.4.1. Culture of Staphylococcus aureus (SA)

At 4 °C, we kept a culture of Staphylococcus aureus (SA) (ATCC 25923) bought from LGC Standards, Middlesex, UK. Bacteria were grown in TSA for 24 h at 37 °C. Pellets of bacteria were collected and resuspended in clean water. Before the antibacterial testing, the optical density was calibrated to a concentration of 1.5×10^7CFU/ml.

2.4.2. In vitro antibacterial activity of CAP-MP's

Researchers used the agar diffusion method to evaluate the efficacy of CAP-MP's against SA to be compared with CAP-only in a study of antibacterial activity. The stock solutions were prepared in DMSO and the solutions were diluted with water. The final concentration of stock solutions for both CAP-MP's and CAP-only was 1 % v/v. TSA was used as the growth medium, and SA inoculum was spread out evenly throughout the surface of the agar in the petri dish before it was sealed. The paper disc contained free CAP and CAP-MP's at a concentration of 2.5 μg/mL. Next, we incubated the Petri dishes at 32 °C for 24 h. Using digital vernier calipers, we determined the size of the inhibitory zone that had formed around the paper discs.

2.4.3. Determination of minimum inhibitory concentration and minimum bactericidal concentration

The microtiter broth dilution method was used to determine the minimum inhibitory concentration (MIC) and minimum bactericidal concentration (MBC) of the tested samples. The CAP-only and CAP- MP's preparations were evaluated. Following the protocol established by the Clinical and Laboratory Standards Institute, the investigation was conducted. At the base of each microplate, we dispensed a bacterial suspension in TSB (100 μL) at a concentration of $1.5x10^7$ CFU/ml. Afterward, we added 100 μL of sample preparations at varying concentrations, with the highest being 7.5×10^6 CFU/mL of bacteria. The plates then spent 24 h in a 37 °C incubator. The minimal inhibitory concentration (MIC) was determined by incubating bacteria at increasing concentrations until growth was suppressed. In addition, 20 μL dilutions of MIC and concentrations above MIC were cultured in TSA plates and incubated at 37 °C for an additional 24 h to determine the MKC. The MKC was found to be the concentration at which 99.9 % of the bacteria died.

2.4.4. Time kill assay

Three independent time-kill assays of CAP and CAP-MP'S were conducted using a modified version of the protocols described in the previous studies (Permana et al., 2021a, 2020a). The SA bacterial suspension was adjusted to 7.5×10^6 CFU/mL by adding dilutions of CAP and CAP-MP'S at concentrations similar to MIC, 2x MIC, and 4x MIC. Twenty microliters of culture mediums were taken at 0, 2, 4, 6, 8, 12, 18, and 24 h after 37∘C incubation. After 24 h of growth at 37 ∘C, the culture was transferred to new TSA plates for cultivation. Finally, the colony forming units (CFU) on the TSA plates were enumerated, and the log CFU/mL was plotted against the time-kill to obtain the curve.

2.5. Preparation of thermoresponsive gel of CAP-MP'S for dermal delivery

The thermoresponsive in situ gel of CAP-MP'S was prepared with various polymer concentrations of Pluronic® F127 and F68 as the preliminary formulation shown in Table 1. Firstly, seven formulations of ratios between pluronic® F127 and F68 were mixed, and the ingredients were combined and stored in the fridge for 12 h. Constant stirring ensured that all of the ingredients were evenly incorporated without any visible lump. The formulation with physiological or even higher (F1-F5) gelation temperature was then put through an affirmation test by the addition of 0.5 % HPMC (Table 2) to see the reduction of gelation temperature compared to the first preliminary formulation.

Table 1
Composition of preliminary formula for CAP-MP's thermoresponsive in-situ gel system.

Compositions	% composition (w/w)						
	F1	F2	F3	F4	F5	F6	F7
Pluronic F127	8	12	16	20	24	28	32
Pluronic F68	2	3	4	5	6	7	8
Gliserin	10	10	10	10	10	10	10
CAP-MP's	1	1	1	1	1	1	1
DMDM Hydantoin	0,1	0,1	0,1	0,1	0,1	0,1	0,1
Distilled water	ad 100	ad 100	ad 100	ad 100	ad 100	ad 100	ad 100

Table 2
Composition of CAP-MP's thermoresponsive in-situ gel formula with the addition of HPMC 0.5 **(%w/w)**.

Compositions	% composition (w/w)				
	F1	F2	F3	F4	F5
Pluronic F127	8	12	16	20	24
Pluronic F68	2	3	4	5	6
HPMC	0,5	0,5	0,5	0,5	0,5
Gliserin	10	10	10	10	10
CAP-MP's	1	1	1	1	1
DMDM Hydantoin	0,1	0,1	0,1	0,1	0,1
Distilled water	ad 100	ad 100	ad 100	ad 100	ad 100

The selected formulation was prepared by dissolving the mixture of ingredients in the water while carefully stirring until a clear solution was achieved; the amount of HPMC added varied depending on the ratios used (Table 3). After that, the in situ thermoresponsive gels were formulated using the same quantity of CAP-MPs as before, which was 1 % w/v of free CAP. All formulations were made in 50 mL as the final concentration.

3. Characterization of thermoresponsive gel of CAP-MP'S

3.1. Gelling temperature measurement (Tsol-gel)

By depositing 2.5 mL of in situ gel in a closed-tube vial and heating it in a water bath set to 20 °C, the sol–gel transition temperature was calculated using a method previously described (Khattab et al., 2019). Every time the bath temperature was increased by 1 °C, the vials were rotated 90°. The temperature at which the gel stops flowing when the vial is turned is known as the Tsol-gel. All the tests were successfully done in triplicates.

3.1.1. Mucoadhesion strength

For this study, we used a modified balancing method to assess mucoadhesive strength. There was rat skin fastened to both the top and bottom of the vials. Between the attached skin (surface area of 2.9 cm^2) 1 g of each gel formulation was placed. Every 30 s, a specific amount of weight was placed on the pan on the right arm of the scale to determine how much pressure was needed to release the gel. The weight was added until the surface of the two vials was split, at which point the process was stopped. The experiment was carried out at a physiological temperature (35°C) in triplicates (Enggi et al., 2021). The equation used to determine mucoadhesive force is described below,

$$\text{Mucoadhesive Strength (N/m2)} = \frac{\text{mg}}{\text{A}} \text{x } 0.1 \quad (8)$$

The m in the equation refers to the mass (gram) needed to release the gel from the skin, g refers to the acceleration due to gravity (980 m/s^2), and A refers to surface area (cm^2).

Table 3
Composition of CAP-MP's thermoresponsive in-situ gel Optimized formula with the addition of HPMC in variety of concentration **(%w/w)**.

Compositions	% composition (w/w)				
	F3a	F3b	F3c	F3d	F3e
Pluronic F127	16	16	16	16	16
Pluronic F68	4	4	4	4	4
HPMC	0,25	0,5	1	1,5	2
Gliserin	10	10	10	10	10
CAP-MP's	1	1	1	1	1
DMDM Hydantoin	0,1	0,1	0,1	0,1	0,1
Distilled water	ad 100	Ad 100	ad 100	ad 100	ad 100

3.1.2. Viscosity

For this purpose, a Brookfield viscometer with an appropriately sized and speeded spindle was used to measure the formulations' viscosities. Thermoresponsive gels were tested at three different temperatures (4 °C, 25 °C, and 37 °C) (Enggi et al., 2021). The viscosity was measured in triplicate using spindle 7 for measurement at 37 °C and spindle 3 for the measurement at 4 °C and 25 °C, with a sample volume of 50 mL and a speed rate of 50 rpm.

3.1.3. Rheological properties

A Brookfield viscometer was used to evaluate the gel's rheological characteristics. Thermoresponsive gels were tested in this experiment at 37°C. Spindle 7 was then used to gradually rotate the gel at 5, 10, 20, 50, and 100 rpm. The dial reading was recorded at each speed. The metric was checked three times.

3.1.4. pH measurement

The pH of the thermoresponsive in situ gel formulation is crucial for patient comfort. The pH levels were tested in triplicate using a digital pH meter from Horiba Scientific in Kyoto, Japan. The pH range must between the acceptable values to ensure comfortable administration.

3.1.5. Spreadability.

Thermoresponsive in situ gel formulation (weighing 500 mg) was spread out on a glass plate and its diameter was measured. Another 500 g glass plate was then placed on the top of the formulation. After 5 min, the diameter of the gel that was spread out was measured (Permana et al., 2020b).

3.1.6. Extrudability

A collapsible tube had 20 g of gel packed inside. The tube was then crimped at one end and clamped to avoid spillage. After taking off the top, the gel began to flow out. The quantity of gel that was extruded was measured with the equation below:

$$(\%)Extrudability = \frac{totalmassofextrudedgel}{totalmassofgelinsertedinthetube} x100\% \quad (9)$$

The percentage done to determine what proportion of the gel was extruded (>90 % extrudability: excellent, >80 % extrudability: good, >70 % extrudability: fair) (Aiyalu et al., 2016).

3.1.7. In vitro skin Occlusive-Ability Evaluation.

The occlusive ability of human skin was tested in vitro using a technique that was previously reported (Malik and Kaur, 2018). The formulation, weighing in at 250 mg, was spread across a sheet of Whatman filter paper (with a pore size of 2.5 ηm). A 100 mL beaker containing 50 mL of distilled water was covered with filter paper that had gel on the top. Filter paper devoid of any formulation was utilized as a control. The beaker contents temperature was maintained at 32 °C, and the system's mass was measured at 0, 6, 24, and 48 h. The percentage of occlusive (C_0) was calculated with the equation below:

$$C0 = \frac{W0 - W1}{W0} x100\% \quad (10)$$

where W_0 represents the water loss in the control group and W_1 represents the water loss in the formulation group.

3.1.8. In vitro hemolytic activity

For the purpose of establishing the CAP-MP's thermoresponsive gel's biocompatibility and safety, an in vitro hemolytic activity investigation was performed. Wistar rats were used to get a recent blood sample. Centrifugation at 2000 rpm for 20 min was used to separate the plasma from the red blood cells (RBC). After three times washes in PBS (phosphate-buffered saline, the RBCs were mixed in a vortex mixer and centrifuged at 2000 rpm for 10 min. A 10 % v/v concentration of PBS was used to resuspend the washed RBC. The samples were evaluated by adding 100 μL to 900 μL of RBC and incubating the mixture at 37 °C for 1 h. Afterward, the samples were centrifuged at 7000 rpm for 10 min. With a UV–vis Spectrophotometer (Dynamica, HALO XB-10), we determined the absorbance of the supernatant at the wavelength of 540 nm. PBS (phosphate-buffered saline) and water (the negative control) were both added to blood samples (Mir et al., 2020). The procedure was replicated three times. Hemolysis was measured using the following formula:

$$Hemolysis(\%) = \frac{(ODtestsample) - (ODnegativecontrol)x100}{(ODpositivecontrol) - (ODnegativecontrol)} \quad (11)$$

3.1.9. Ex-vivo skin dermatokinetic study

The skin was manually implanted with the CAP-thermoresponsive MP's gel and then attached to Franz cell diffusions with cyanoacrylate glue for evaluation of ex vivo dermatokinetics. Receptor media consisted of PBS (pH 7.4) with 1 % w/v Tween 80. On top of the gel, a 5 g cylinder of stainless steel was placed. The speed of 600 rpm was used and the environmental temperature was set at 37 ± 1 °C in the experiment. in the experiment. After being removed from the gel and washed with PBS, the skin samples were obtained at regular intervals. Next, a 5 mm biopsy punch was used to make a hole in the patient's skin (Stiefel, Middlesex, UK). The samples of skin were heated in a water bath at 60 °C for two to three minutes in order to separate the epidermis and dermis. Forceps were used to gently separate the epidermis from the dermis. Afterward, 1 mL of methanol was added to the skin sections, and the resulting mixture was homogenized using a Tissue Lyser LT (Qiagen, ltd., Manchester, U.K.) at 50 Hz for 10 min to extract CAP from the skin. To find out how much CAP there was entrapped there, HPLC was used for further analysis. In addition, the use of a one-compartment open model, PKSolver (China Pharmaceutical University, Nanjing, China) was used to create a curve of the drug concentration vs time of application. Afterward, the dermatokinetic profiles were calculated. The drug maximum concentration (Cmax), time to achieve maximum concentration (tmax), area under the curve from time zero (t = 0) to the last experimental time point (t = 24 h) (AUC), mean of drug half-life ($t^{1/2}$), and mean residence time of the drug (MRT) were all determined. The CAP conventional gel was also evaluated dermatokinetically as a comparison (control).

3.1.10. Ex vivo antibacterial activity using bacterial infection model on rat skin

3.1.10.1. Preparation of bacterial skin infection model. For sterilization, the skins were submerged in 70 % ethanol for 1 h. After washing, the skin was dried for 20 min in a biosafety cabinet. To recap, 50 μL of the 1.5×10^7 CFU/mL bacterial solutions were injected intradermally into the sterile skin. The sections of skin were sterilely placed on TSA plates. Every day, for 7 days, the plates were transferred aseptically to new TSA plates at 37 °C while the skin was being cultured.

3.1.10.2. Determination of ex vivo antibacterial activity using bacterial infection model on rat skin. A Similar apparatus on the dermatokinetic evaluation was also used to test the antimicrobial efficacy of the compound in an ex vivo bacterial infection model using rat skin. In this experiment, the skin infection model was established in Franz diffusion cells rather than using normal full-thickness rat skin. Skin samples were taken 6, 12, and 24 h after CAP- MP's thermoresponsive gel was applied, and 1.5 mL of sterile water was applied to each sample in a microtube. Then, for 15 min, the mixture was homogenized using a Tissue Lyser LT (Qiagen, ltd, Manchester, UK) at 50 Hz. Finally, TSA plates were inoculated with 20 μL of the homogenized samples and incubated for 24 h at 37 °C.

Additionally, the same technique was carried out using both a placebo gel and a standard gel containing CAP on the affected area. To conclude, the total number of viable colony-forming units (CFUs) was determined. As a comparison, we used infected skin that had not been treated with any gel or CAP composition.

3.2. Statistical analysis

Statistics were presented as means ± standard deviation (SD). Microsoft® Excel® 2016 was used to calculate the mean, standard deviation, linear regression analysis, percentage RSD, and coefficient of variation for each sample used in the validation technique (Microsoft Corporation, Redmond, USA). Data were analyzed statistically using GraphPad Prism® version 6 (GraphPad Software; San Diego, California, USA). For which a statistically significant difference was indicated when the p-value was<0.05 (p-value < 0.05).

4. Results and discussion

4.1. Physicochemical determination and characterization of chloramphenicol encapsulated whey protein microparticle (CAP-MP's)

The formulation of Chloramphenicol microparticles (CAP-MP's) was developed to enhance the physicochemical characteristics and the skin penetration of CAP-MP's. In order to evaluate whether our findings showed desirable properties, several evaluation procedures were developed in the present investigation. The microparticle formulation used a thermal cross-linking procedure of denatured WPI proteins according to a modified water-in-oil emulsion method (Wu et al., 2015). For this purpose, fourteen formulations were established and four parameters were evaluated between formulas, where the F1-F5 were the variety of CAP concentrations, F6-F8 were the variety of WPI concentration, F9-F11 were the variety of mixing speed (rpm) and F12-F14 were the variety of mixing times. All formulas were used to observe the effect on each parameter to produce better properties of microparticles and all the parameters were summarized in Table 4.

4.1.1. Size determination of particles, zeta potential and PDI

When it comes to the development of stable formulations, the particle size and zeta potential of micro-encapsulated compounds can provide invaluable insight. The particle size of CAP-MP'S with the fourth parameter can be seen in (Fig. 1). The mean particle size values of CAP-MP'S in the F1-F5 (various concentration), F6-F8 (various WPI concentrations), F9-11 (Various mixing speed) and F12-F14 (various of mixing times) were 0.95 ± 0.07 μm; 0.98 ± 0.11 μm; 1.12 ± 0.11 μm; 1.11 ± 0.14 μm; 1.14 ± 0.16 μm; 0.35 ± 0.06 μm; 2.23 ± 0.03 μm; 6.01 ± 0.19 μm; 8.95 ± 0.19 μm; 7.40 ± 1.13 μm; 2.17 ± 0.07 μm; 5.62 ± 0.38 μm; 2.01 ± 0.07 μm; and 2.06 ± 0.10 μm, respectively.

The main composition of WPI is β-lactoglobulin which is known to have the ability of binding hydrophobic complexes by their binding sites at a pH of 7.0, permitting ligands to reach the hydrophobic core and so facilitating the binding of a significant number of extremely small hydrophobic molecules (Wang et al., 2019) Chloramphenicol is a hydrophobic compound that works with proteins in making smaller and more

Table 4
Specifics regarding the formulation parameters that went into the making of CAP-MP's.

Formulation Code	CAP in PG (ml)	SPAN in VCO (%)	WPI in water (%)	Total amount of CAP in the mixture (mg)	Mixing Speed (rpm)	Mixing time (minute)
F1	2	5	10	25	5000	10
F2	2	5	10	50	5000	10
F3	2	5	10	100	5000	10
F4	2	5	10	200	5000	10
F5	2	5	10	400	5000	10
F6	2	5	5	100	5000	10
F7	2	5	15	100	5000	10
F8	2	5	20	100	5000	10
F9	2	5	15	100	1250	10
F10	2	5	15	100	2500	10
F11	2	5	15	100	7500	10
F12	2	5	15	100	5000	5
F13	2	5	15	100	5000	15
F14	2	5	15	100	5000	20

compact particles due to its strong hydrophobic interaction (Wang et al., 2019). The excellent emulsification ability of WPI, which acts as a surfactant because of its hydrophilic and hydrophobic areas, could produce smaller microparticles than those of other proteins (Shen et al., 2018).

Larger particle size was seen at greater drug concentrations due to the ability of β -lactoglobulin to entrap or absorb drug components, resulting in a stronger hydrophobic contact. The particle size also depends on the increasing amount of WPI, which can be seen in Fig. 1B. When compared to other parameters of formulation, there was an increase of the particle size that was found to be significantly higher ($p < 0.05$) due to the higher concentration of WPI in the formulation. There were core-coating ratios between the drug entrapped in WPI. At a different speed of mixing (1250 to 7500 rpm), small droplets ranging from 200 to 800 μm were obtained and showed a significant difference ($p < 0.05$) that is clearly shown in Fig. 1C. As the mixing speed increased, the size distribution become narrower. This is due to gravity's diminishing pull, the system may be able to stay together without showing signs of dissociation, coalescence, or flocculation which is suggest that the stability of microparticle formulation can be significantly impacted (Tadros et al., 2004). Comparing the fourth parameter in the formulation, CAP-MPs produced at 7500 rpm with a particle size of 209 μm were chosen as a suitable formulation for further examination.

Fig. 1 also illustrates the polydispersity index (PDI) values for all formulations and parameters. The presence of microparticles with higher PDI values points to a broad size distribution, which indicates that the substance is more susceptible to Ostwald ripening. A lower PDI value close to zero, on the other hand, suggests that there is homogenous dispersion between particles and a relatively narrow distribution with

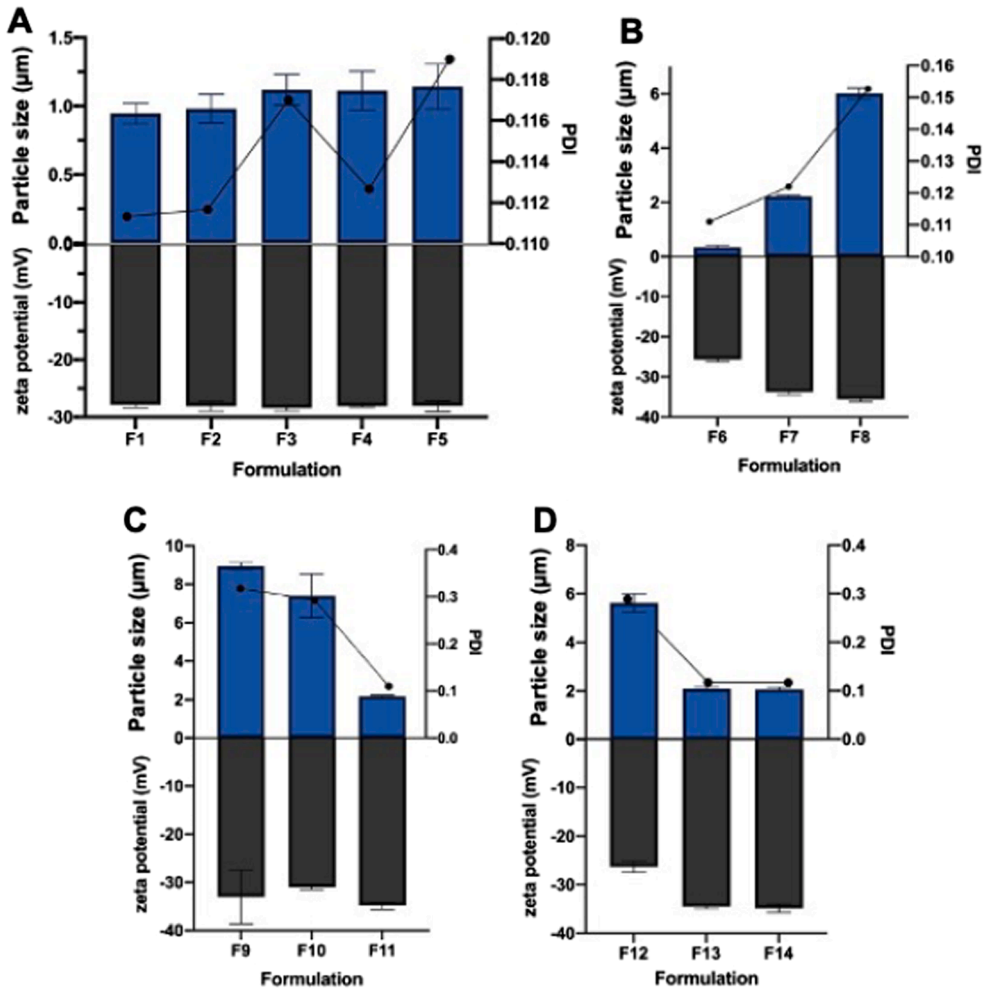

Fig. 1. Particle size, zeta potential and PDI value for the variety of drug concentration (F1-F5) (A); Particle size, zeta potential and PDI value for the variety of WPI concentration (F6-F8) (B); Particle size, zeta potential and PDI value for the variety of mixing speed (F9-F11) (C); Particle size, zeta potential and PDI value for the variety of mixing time (F1-F5) (D).

strong physical stability (Wang et al., 2019). The PDI in F1-F5 had a variation in drug concentration that did not experience a significant difference, as well as the addition of polymer concentration (WPI) in the F6-F8 formula ($p > 0.05$). The PDI value was different in F9-F11 which was influenced by the mixing speed and found to be significantly different ($p < 0.05$) because the size distribution was narrower with the increase in the speed of mixing. This is what happened in F1-F8 where there was no significant difference; the speed used for the eighth formula was 5000 rpm which caused the PDI values to be approaching the F11 formulation (0.111 ± 0.006). The same theory also supports a significant difference in F12-F14 with variations in mixing times; when mixing at 15–20 min at 5000 rpm, it also showed a PDI that is close to zero, similar to F1-F8 and F11 (Fig. 1). Higher speeds and mixing times lead to a smaller PDI value (PDI > 1), which may be attributable to the increased interaction between WPI and CAP. This interaction leads to a more homogeneous particle system with a narrower size dispersion and no aggregation potential between particles (Shen et al., 2018). By observing the variety of PDI values between all parameters, we can establish that the uniform particles could be obtained if the mixing speed was in the range of 5000–7500 rpm with a mixing time between 10 and 20 min. For this reason, we choose the F11 formulation with mixing speed and time at 7500 rpm and 10 min, respectively.

The determination of CAP-MP'S zeta-potentials was also presented in (Fig. 1). Observations of the zeta potential provide a value that indicates the intensity of the force that acts to repel particles from one another. Both the composition of the microparticles and the medium in which they were scattered and had an effect on the zeta potential. Because the pH was thought to be greater than the isoelectric point of whey protein, the zeta potential value for the entire substance has a tendency to be negative. When the pH was greater than the isoelectric point, which happens when the pH was above 5, proton dissociation takes place. The dissociation results in the particle having a negative charge. The significant difference in F6-F8, which was affected by the addition of polymer, was due to the charge carried by each polymer. As more of the polymers were added, the tendency for the zeta potential to increase will also occur; this change results in greater forces of repulsion between particles and has the potential to improve the physical stability in a variety of systems (Muller, R.H.; 1996). The dispersion of the charge

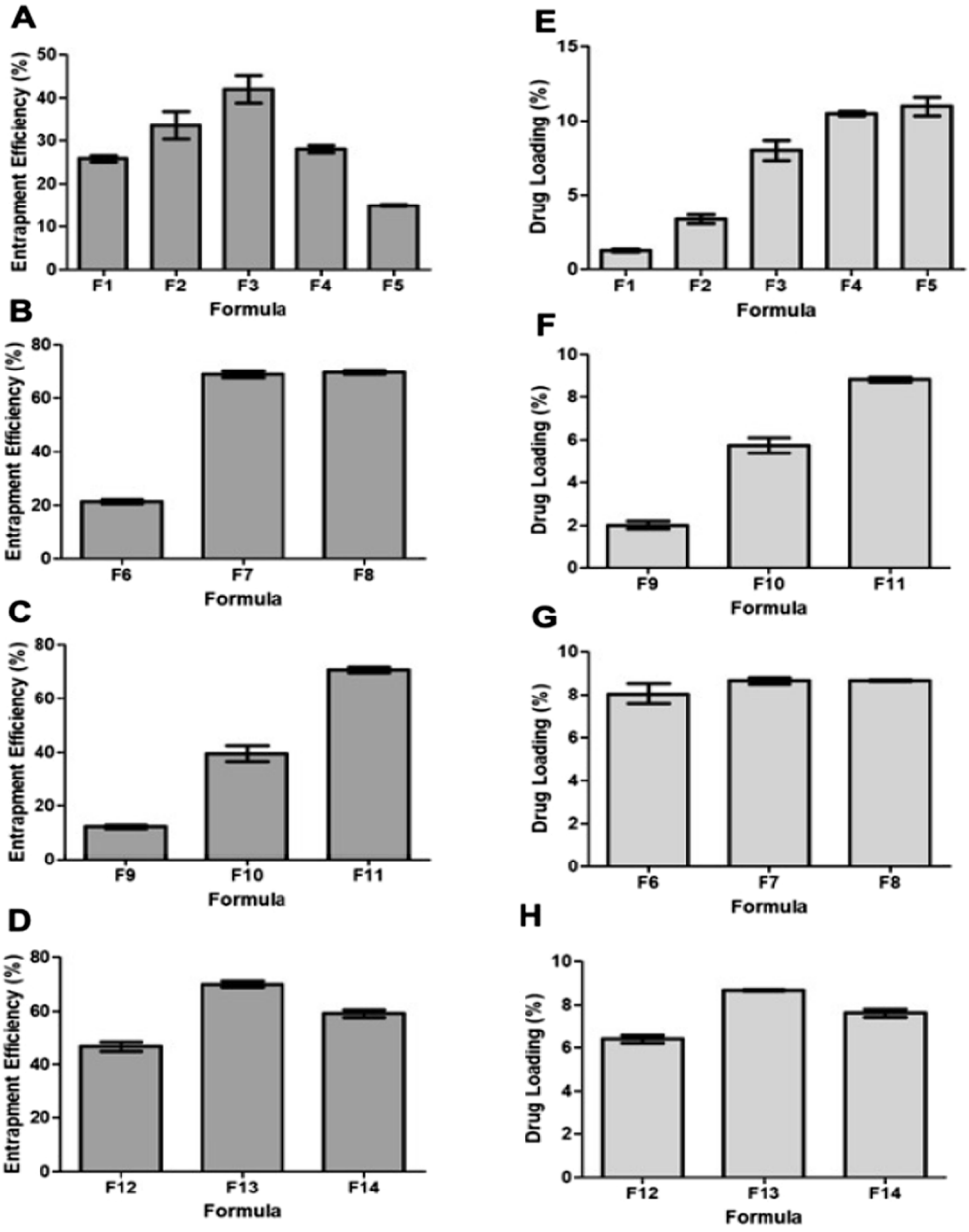

Fig. 2. Entrapment efficiency for the variety of drug concentration (F1-F5) (A); Entrapment efficiency for the variety of WPI concentration (F6-F8) (B); Entrapment efficiency for the variety of mixing speed (F9-F11) (C); Entrapment efficiency for the variety of mixing time (F1-F5) (D). Drug Loading for the variety of drug concentration (F1-F5) (E); Drug Loading for the variety of WPI concentration (F6-F8) (F); Drug Loading for the variety of mixing speed (F9-F11) (G); Drug Loading for the variety of mixing time (F1-F5) (H).

in the microparticle mixture was also affected by the speed of the mixing as well as the duration of the mixing. This effect suggests that CAP may be attached to WPI microparticles. Wang et. al. reported a similar finding, where zeta potential values dropped after the encapsulation of CAP into β -lactoglobulin from −8.63 to −17.93 mV (Wang et al., 2019). This was the reason why the negative charge of the particles in our findings was increasing between F9 and F11 from –33 to −34 mV due to the higher speed and time of mixing and F11 was chosen as the formulation for further evaluation.

4.1.2. Encapsulation efficiency (EE) and % drug loading

The percentage of encapsulation efficiency and drug loading was measured according to the derivatization method explained in section 2.3.2. This evaluation demonstrated how well CAP was encapsulated into WPI microparticles. While adding CAP to WPI microparticles at the highest concentration (200 and 400 mg), encapsulation effectiveness was found to decrease (Fig. 2A). The decrease indicates that some of CAP components were not embedded but rather floated freely in the protein matrix. Similarly, Patel et. al. showed that the %EE of protein nanoparticles containing curcumin (hydrophobic compound), which were thought to be precipitated, reduced as the concentration of curcumin increased (Patel et al., 2010).

For the samples with encapsulation efficiencies higher than 60 %, it was affected by the ratios of WPI to CAP, higher speed, and time of mixing. The adsorption efficiency increased when the emulsification rate and duration of emulsification were increased and the evaporation time induced by heating was also increased (80 °C). Faster emulsification would cause smaller emulsion globules, which in turn would permit the production of smaller particles. More energy was produced during the homogenization process, hastening the dispersion of the polymeric organic phase, and resulting in particles that are both exceptionally small and uniformly distributed. The inability to adequately disperse the organic phase may account for the bimodal distribution observed at homogenization rates of 1250 and 7500 rpm (Sharma et al., 2016). Previous research has also shown that astaxanthin encapsulated in whey protein isolate generally had an EE percentage of>90 % across the board (Shen et al., 2018).

With a high drug loading capacity, a good microparticle system can use less of the matrix material in the treatment. Drug loading and entrapment efficiency were significantly impacted by polymer composition, molecular weight, drug interaction between polymers, and the presence of end functional groups (ester or carboxyl). Maximum adsorption and minimum solubility occur at or near the isoelectric point when the loading efficiency of the macromolecule or protein was highest. Ionic interaction between the drug and matrix materials has been shown to be a very effective approach to boosting drug loading, especially for small particles (Shahi & Thube, 2011). Drug loading, based on the observations of the variation of drug concentrations, experienced a significant difference ($p < 0.05$) because the greater the drug concentration, the higher the measured drug concentration in the mixture of microparticles (Fig. 2E). The effect of adding polymers in with the microparticles will also increase drug loading, which affects the amount of precipitate that will be measured from the overall weight of the mixture (Fig. 2F). This was based on the influence of stirring speed and stirring time, which is both influenced by the increase in sorption efficiency. Sorption efficiency will also affect drug loading. In F14, the drug loading decreased because the mass of the precipitate, which affected the total weight in the formulation, also decreased so that the measured drug levels would also be relatively low. The yield of nanoparticles will also decrease with the increasing stirring speed. A study conducted by Permana et al. incorporated Itraconazole into NC's, which was supposed to intensify the dispersibility between particles, including those in aqueous polymeric solutions (Permana et al., 2021a).

Based on the explanation above, the formulation code F11 was used as further consideration for the next characterization by paying close attention to the mixing time and speed of 10 min and 7500 rpm, respectively, as well as the WPI concentration of 15 % and 100 mg CAP concentration in the mixture. The formula was chosen specifically because it can produce small particles at 2.17 ± 0.07 μm with a lower PDI value close to zero (0.111 ± 0.006) and a negatively charged particle with a zeta potential value of -34.84 ± 0.77 mV, indicating a good attachment process of CAP to WPI microparticles. The F11 formula also had a higher drug entrapment efficiency (%EE) than the other formulas, measuring at 70.64 ± 1.12, and a huge proportion of drug loading which is found at 8.8 ± 0.12.

4.1.3. SEM analysis

The F11 formulation prepared at a mixing speed of 7500 rpm was further evaluated using a light microscope and SEM as depicted in Fig. 3 (D) and 3(E). Both evaluations showed the same characteristic of CAP-MP's. They have a smooth, spherical particle shape with a particle range that starts at 200 μm. WPI microparticle preparation has the potential benefit of increased heat stability as a result of pre-heating, making it preferable to WPI molecules on an individual basis for applications that call for heat treatment (Sağlam et al., 2013). Hydrophobic microdomains may also be exposed due to heat-induced protein unfolding. This would result in a somewhat hydrophobic and hydrophilic surface on the WPI microparticles, enabling their application in emulsions. Because WPI microparticles near the o/w interface contain charged proteins, they prevent the emulsion droplets from aggregating by electric repulsion and coalescing via steric contact (Wu et al., 2015). Same to what we already observed, Khan et al. also observed smooth, spherical, and more apparent shape particles when observing particles that were encapsulated with whey protein (Khan et al., 2019). Microparticles being able to enter human skin was affected by factors such as particle size and formulation. Particles>1 μm tend to remain on the skin's surface, where they might gather into films. Only a small fraction of microparticles manage to pass through the lipid layers of the stratum corneum; those with a diameter of<1.5 μm were able to efficiently reach a depth of>2 μm within hair follicles. Microparticles were able to penetrate the hair follicle's lipid bilayer, allowing for better medication delivery (Lademann et al., 2004).

4.1.4. FTIR evaluation

The FT-IR spectra in Fig. 3A illustrate the interaction between WPI and CAP in a CAP-MP's followed by the physical mixture of CAP and WPI (1:1), and in WPI and CAP alone. Noteworthy peaks in the infrared spectra were seen between 3200 and 3600 cm^{-1}, which were interpreted as signs of hydrogen bonding (Teng et al., 2013). After being encased in WPI microparticles, however, the O—H functional groups (3489 cm^{-1}) in the CAP peak were still seen at the same wavelength, which is thought to be the main facilitating force for microparticles production (Bagheri et al., 2013). It was discovered that the spectra of CAP, the physical mixture, and the CAP-MP's have a number of characteristic peaks at 2974 cm^{-1} that were attributable to C—H stretching of the aliphatic group (Khan et al., 2019). Whey protein isolate consists primarily of the proteins α-lactalbumin and β -lactoglobulin. Their existence is confirmed by the presence of Amid I and Amid II bands, which are sometimes referred to as the "backbone" of WPI. The Amid I bands were found in the encapsulated CAP between 1600 and 1800 cm^{-1}, which are predominantly attributed to carbonyls with C═O stretching vibrations. The 1453 cm^{-1} absorption bands seen in Amid II were related to a structure that combines a C—N stretch and an N—H bending group deformation of protein isolate (Goyal et al., 2015). The addition of WPI did not cause a shift in the wavelength of CAP in the CAP-MP's spectrum. However, it did increase the intensity of the absorbance, suggesting that the N—H group of the CAP was introduced to the exposure of the peptides, and the interaction between WPI and CAP was likely electrostatic rather than chemical reactions (Wang et al., 2019).

It appears that electrostatic forces were responsible for the interaction between WPI and CAP (Dai et al., 2016). A rise in the strength of Amid I and Amid II was also suggestive of the binding of CAP to β

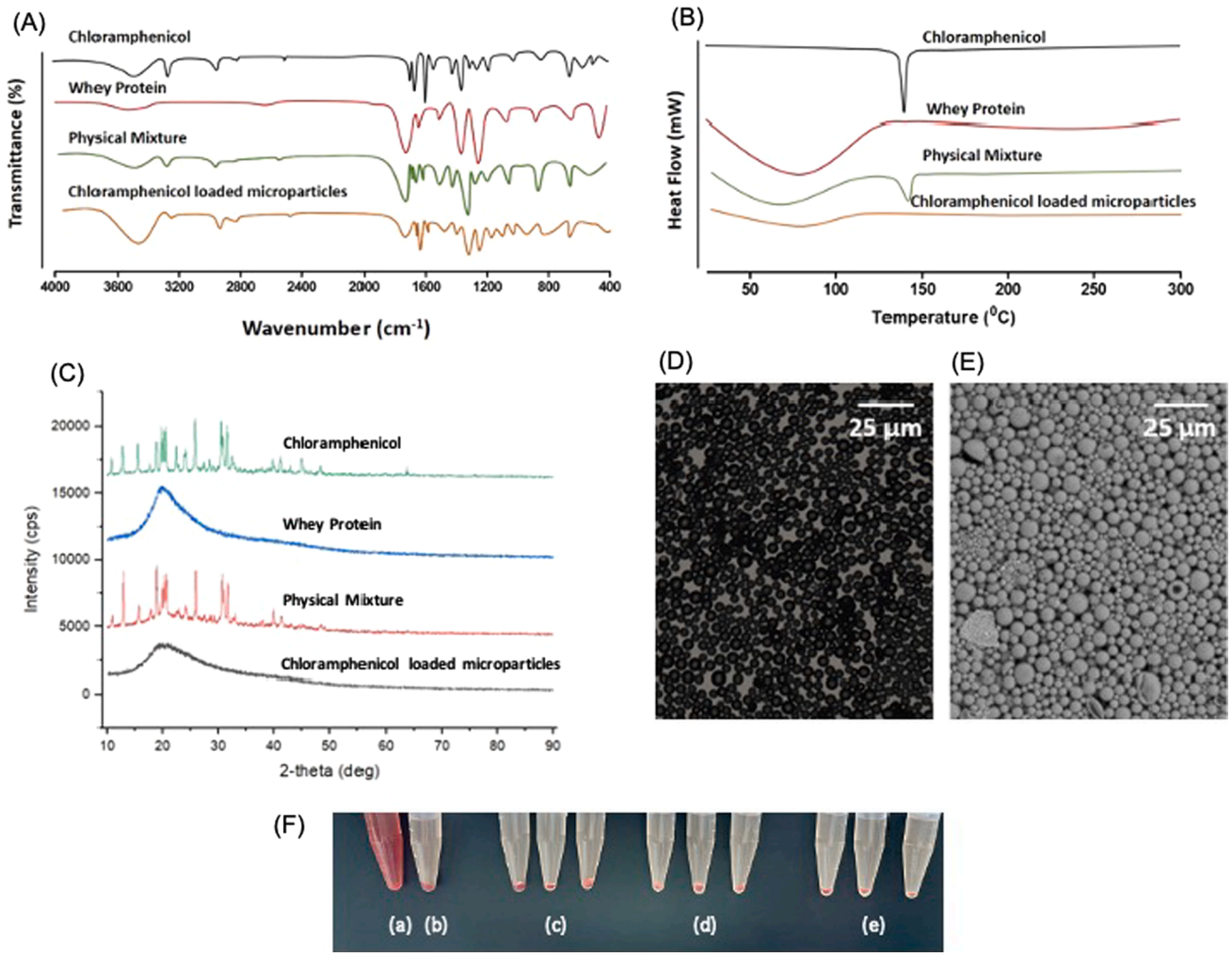

Fig. 3. Representative image for FT-IR (A); DSC (B); XRD (C); light microscope (D) SEM (E) (The white scale exemplifies a length of 25 µm in each measurement), Hemolytic assay (F) of negative control (a), positive control (b), group of 500 ppm (c), group of 50 ppm (d), group of 5 ppm (e).

-lactoglobulin. Research by Hasni et. al. detected that the intensities of Amid I and Amid II both increased, but there was no substantial shifting after the binding of lipids to β -lactoglobulin (Hasni et al., 2011). Changes in the secondary structure were detected by Amide I and Amide II (Jia et al., 2016). Intensity shifts demonstrated how CAP affected the secondary structure of β -lactoglobulin, which is consistent with spectral findings. For the most part, the interaction between a protein and a small particle of hydrophobic material was thought to be mediated via hydrogen bonding and hydrophobic force.

Hydrogen bonds were frequently implicated in hydrophilic interactions involving C═O, N—H, and C—N. The hydrophobic interaction and the -C—H antisymmetric stretching vibration were both associated with the wavelength region of a 2900–3000 cm^{-1} absorption band (Hasni et al., 2011). Variations in the intensity indicated the involvement of the hydrophobic interface between the β -lactoglobulin in whey protein and CAP complexes.

4.1.5. DSC evaluation

Whey protein isolate, CAP microparticles, native chloramphenicol, and a 1:1 CAP:WPI physical combination were all depicted on the DSC thermograph from 20° to 300 °C in Fig. 3B. In both the WPI-only and CAP-MP's DSC curves, an endothermic peak between 50 and 120 °C was seen, with the peak temperature centered at ± 80 °C. In contrast, the WPI-only and CAP-MP's samples showed no melting point, showing that the CAP was amorphous in the monodispersions. The findings agreed with the study of Yi et al., who reported that protein-based and protein-dextran-conjugated nanoparticles encapsulating β-carotene were also amorphous (Yi et al., 2015) Whey protein's primary components, α -lactalbumin, and β -lactoglobulin, undergo heat-induced transitions, which may contribute to the endotherm quality. Moreover, between 140 and 150 °C, an endothermic peak developed in the physical mixture of WPI and CAP (1:1).

This may be due to the evaporation of absorbed water. At around the melting point of 149 °C, sharp peaks were detected in CAP-only. In the CAP-MP's and WPI-only samples, only an endothermic peak was seen, indicating that the CAP was correctly encapsulated in the WPI microparticles and molecularly disseminated in the polymeric matrix.

It is important to compare our findings to other hydrophobic components, such as zein, ergocalciferol, and cholecalciferol nanoparticles studied by Luo et. al., by showing the lack of endothermic peaks of zein and CMCS lacking endotherm peaks; this indicates that the zein was molecularly dispersed in the polymeric matrix and confined inside the CMCS-calcium matrix, which means it was encapsulated inside the nanoparticles (Luo et al., 2012). A similar discovery was made by Lai and Guo, demonstrating that the lack of an endotherm peak in analyzed temperatures was proof of encapsulation (Lai and Guo, 2011).

4.1.6. Xrd

The samples' crystallinity was measured in order to draw conclusions about their respective properties by utilizing X-ray diffraction (Silva et al., 2016). To determine the structural properties of the dry products of CAP microparticles as an essential component of the

examination we observed the broadband X-ray diffraction patterns, or those with a larger peak pattern, as an indication of amorphous structures because the molecules in this condition scatter light more widely (Silva & Meireles, 2015). Fig. 3C displays powder X-ray diffraction patterns derived from the CAP-MP's and the raw materials employed as the drug and polymer. In good agreement with the DSC thermograms, the XRD evaluations showed distinguishable peaks around the 20–35 °2θ regions with a large, diffuse peak that can be clearly seen in the diffractograms, indicating that the CAP enclosed with WPI had an amorphous structure. The absence of a common peak between the raw materials (CAP) and the CAP-MP's generated suggests that the CAP was encapsulated with WPI prior to particle production. When an amorphous matrix undergoes a transition from its vitreous state to its gum state, which may happen with a rise in moisture content or at elevated temperatures, the encapsulated hydrophobic chemicals are released (Ordoñez & Herrera, 2014).

4.1.7. In vitro drug released studies of CAP-MP's

The curve in Fig. 4A showed the comparison of drug release between CAP-only and CAP-Mp's. To suit the physiological conditions of the skin, in vitro drug testing was performed using simulated wound fluid. Based on this research, it can be seen that the drug encapsulation process into microparticles using whey protein can improve the drug release profile. The study showed that the percentage of drug released from chloramphenicol microparticles after 24 h was 95.85 ± 2.30 %. Drug release of CAP-MP's at 8 to 24 h was rapid and stagnant. On the other hand, the amount of a single chloramphenicol drug was 96.51 ± 2.92 % after only 6 h. The formulation of chloramphenicol in the form of microparticles was able to show a continuous pattern with observation for 24 h, different from the use of CAP-only which showed a faster release profile and reach approximately 100 % release only in 6 h. This profile was related to the curved surface area of chloramphenicol and did not show a lead curve as a sign of drug enhancement, with a controlled release profile (Lee & Choo, 2015). The release of the drug from the encapsulated polymer could occur because CAP has a weak bond to the polymer matrix (whey protein). The solubility of WPI in simulated wound fluid also plays a role in the drug release process so that it can cause erosion of the microparticle matrix which causes prolonged drug release.

4.1.8. Drug release kinetic using mathematical modelling

The data of drug dissolution was analyzed with five different kinetic

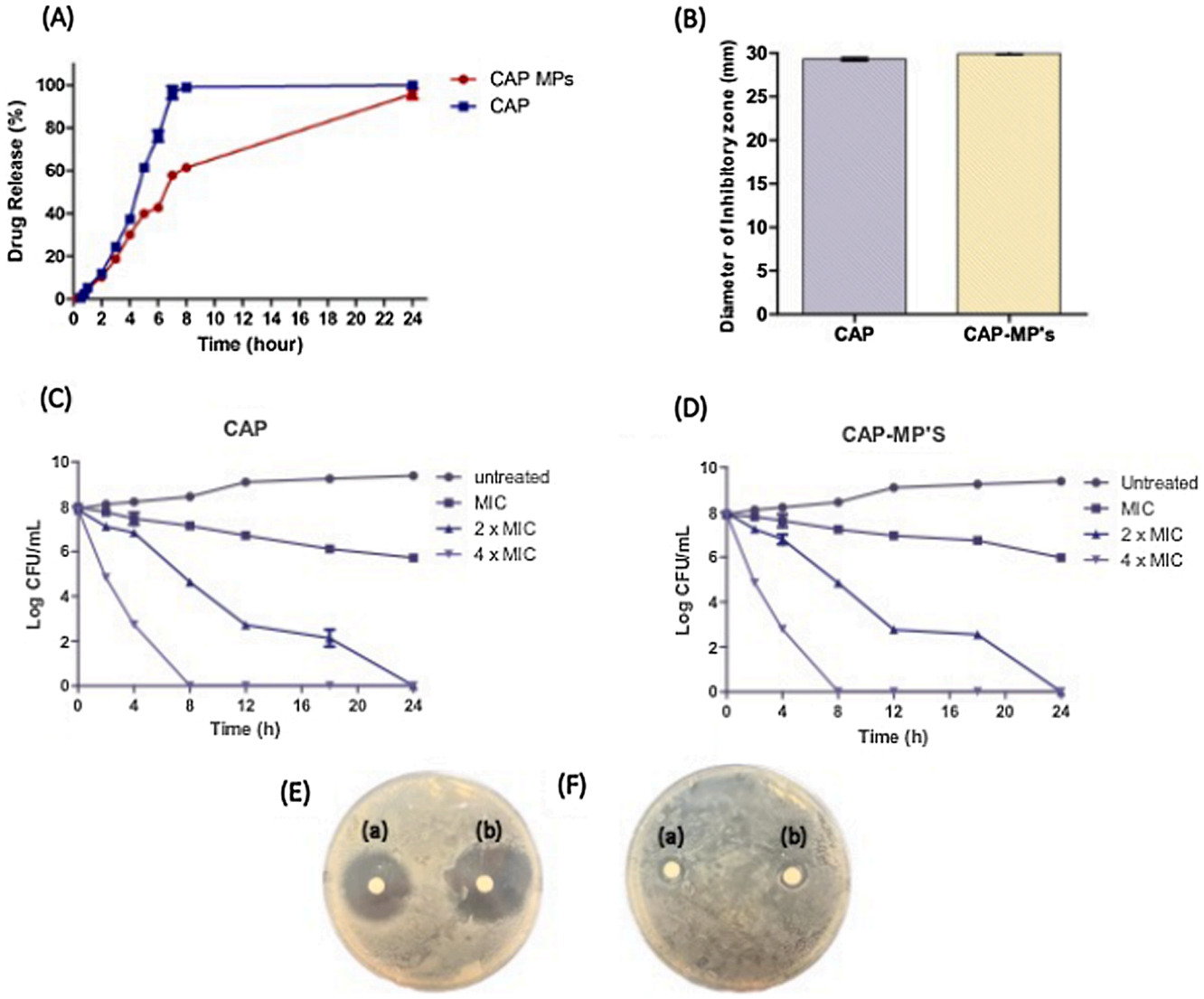

Fig. 4. % Drug release of CAP-MP's compared to CAP-only (A); Diameter of inhibitory zone formed against SA of CAP-only and CAP-MP's (B); Time Killing Assay for CAP-only (C); Time Killing Assay for CAP-MP's (D); The inhibitory zone (E) of CAP-only (a) and CAP-MP's (b); The inhibitory zone of controls (F), (mean ± SD, n = 3).

models to investigate the dissolving mechanism and kinetic modeling of CAP and CAP microparticles (F11). The model with the highest coefficient correlation was chosen as the best fit for the release process. The results revealed that the release profiles of microparticle formulations (CAP-MP'S) were following the Hixson Crowell model, while that of CAP-only followed zero order models with R values of > 0.97 (Table 5). The Hixson-Crowell kinetic models describe particle release from systems with changes in particle surface area and diameter. For a drug consisting of uniformly sized particles, it was possible to derive an equation that expresses the rate of dissolution based on the erosion ability of the matrices to release the drug. Hence, it can help to define the release pattern of the drug as it governs the efficacy of the dosage form. In conclusion, we can say that drug release of SDF-loaded polymer matrices follows an erosion mechanism (Arafat et al., 2021; Singhvi & Singh, n.d.).

Statistical analysis shows that CAP-MPs have a considerably greater percentage of dissolution profiles compared to CAP-Only ($p < 0.05$), this can be clearly seen at Fig. 4A.

4.2. In vitro antibacterial activity

4.2.1. In vitro antibacterial activity of CAP & CAP-MP's

The purpose of this analysis was to compare the antimicrobial efficacy of CAP-only and CAP- MP's treatments against SA. Fig. 4E shows the results of the inhibitory zone between the two samples. The inhibition zone diameter of CAP samples was 29.2 ± 1.76 mm and increased to 30.05 ± 0.65 mm in CAP-MP's sample (Fig. 4B). The results demonstrate that the formulation of CAP into microparticles was able to improve the antibacterial activity, even if did not significantly increase ($p < 0.05$). Therefore, there was no discernible distinction in inhibitory zone diameter between CAP and CAP- MP's. ($p < 0.05$). Results were found in DMSO (1 %) and the control did not show any inhibitory zone (Fig. 4F). More efficient drug diffusion into the media and deeper penetration of microbial cell membranes would result from improved solubilization and decreased CAP microparticle size (Niwa et al., 2015). The greater amount of free CAP in the dispersion media may potentially contribute to the expansion of the inhibition zone produced by the CAP-MP's formulation. This further verifies that the drug used must be in soluble form for its antibacterial activity to be displayed.

4.2.2. Minimum inhibitory concentration (MIC) and minimum bactericidal concentration (MBC) evaluation

The MIC and MBC values of CAP-only and CAP-MP's were presented in the same manner as in Table 6. This once again confirms that the formulation of CAP into MP's did not have any interruption to reduce or even increase the MIC and MBC value of pure CAP, which means that, in order to increase the solubility, it was possible that any therapeutic medicine that requires this substance will take benefit from it.

4.2.3. Time Killing assay

Fig. 4C and 4D show the CAP-only and CAP-MP's time-kill curves against SA in terms of time. The time taken for an antibacterial treatment to completely remove bacterial growth was measured in this experiment. Following 24 h of growth, the viable SA colony in the untreated group reached 9.3 ± 0.08 log CFU. The results also show that neither CAP nor CAP-MP'S were able to kill 99.9 % of SA at MIC value. After 18 and 24 h of incubation with 2x MIC, CAP and CAP-MP's showed no signs of viable SA. Moreover, a concentration of 4x MIC resulted in a quicker killing time, which was discovered at 8 h of incubation for both CAP and CAP-MP's. These results suggest that CAP's antibacterial activity declines with increasing concentration and prolonged exposure (depending on concentration and time). The solubility of CAP in bacterial culture media was also highlighted for its potential as an antibacterial agent.

Table 6
MIC and MBC of CAP-MP's and CAP-only against SA (n = 3).

Sample	MIC (mg/ml)	MBC (mg/ml)
CAP	12.5	25
CAP-MP's	12.5	25

4.3. Characterization of thermoresponsive gel preparations incorporated CAP-MP'S

Several methods can be used to identify what makes a thermoresponsive in situ gel effective in delivering drugs to the dermal layer of the skin. The gel-forming polymer was a key ingredient in the formulation. For the purpose of this research, a thermoresponsive in situ gel was formulated using a tri-polymer blend consisting of Pluronic® F127, Pluronic® F68, and HPMC. Poloxamer, or Pluronic®, was a triblock copolymer made up of hydrophilic ethylene oxide (EO) and hydrophobic propylene oxide (PO). As a result, additional polymers including Pluronic® F68 and HPMC were frequently used in the formulation to enhance the gel properties (Kurniawansyah et al., 2020). Gel formation was likely to be sensitive to polymer concentration due to the fact that different polymers have varying chemical characteristics. For the formulation optimization, seven formulas were used as preliminary to determine the ratios between Pluronic F127 and F68 in gel formation based on the best characteristic of dermal delivery. After finding the best formula from the preliminary by measuring the gelation temperature and bioadhesive strength, HPMC was added at a concentration of 0.5 %. The chosen formula was optimized by varying the HPMC concentration to determine the best formula for further evaluations. Responses were logged for in situ gel properties such as gelation temperature (Tsol-gel), mucoadhesion strength, viscosity, pH, viscosity, rheology, extrudability, hemolytic assay, and ex vivo drug penetration.

4.3.1. Gelation temperature evaluation (Tsol-gel)

When creating a thermoresponsive gel, the gelation temperature (Tsol-gel) was a crucial factor. A correct dose can be delivered if the formulation of the thermoresponsive in situ gel allows it to remain liquid at room temperature. The acceptable range of Tsol-gel for thermoresponsive in situ thermoresponsive gel should correspond to the average skin temperature, which is between 32 and 37 ∘C (Tang et al., 2013). The temperature at which the liquid became a gel was calculated using the inverted tube method. Fig. 5 shows exemplary photographs of a thermoresponsive gel formulation at room temperature (liquid) and at body temperature (gel).

The seventh formulation in the preliminary formula exhibits widely varying Tsol-gel values, with the highest gelation temperature being seen in the F1-F2 formulations at>60 °C (Fig. 6A). According to the results of the analysis, the gelation temperature was significantly affected by the ratio of Pluronic® F127 to F68. When comparing the formulation of F1-F2 with F3-F7, it has a lower degree of gelation

Table 5
Representative Kinetic model of drug release between CAP and CAP-MP's.

Sample	Kinetics Model				
	ZO	FO	Higuchi	KP	HC
CAP	0.978875349	0.713857175	0.756758792	0.963510593	0.916960875
CAP-MP's	0.793739921	0.965534225	0.873949568	−0.61299788	0.974923098

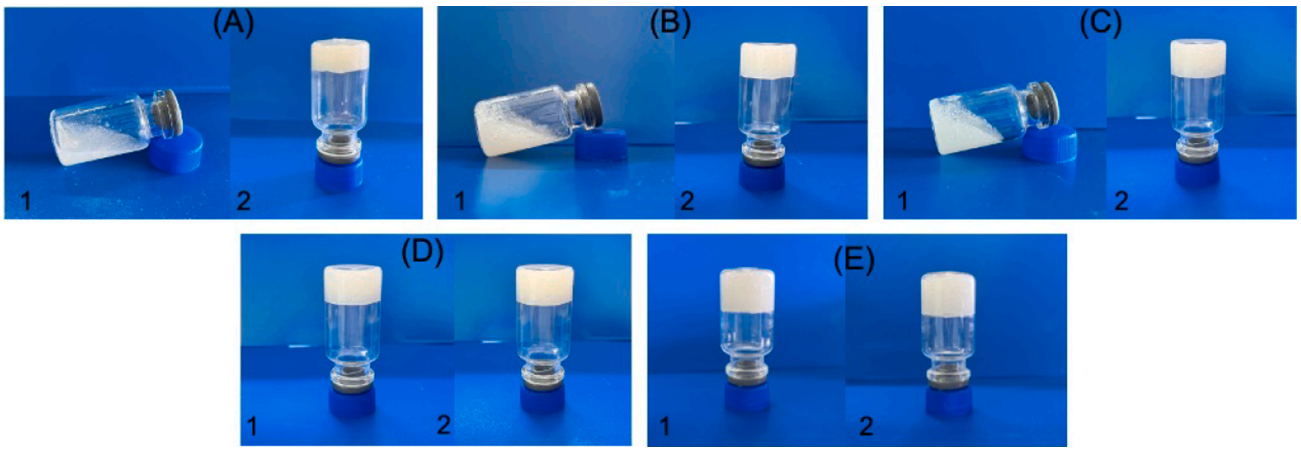

Fig. 5. Gelling properties for optimized formulation of F3a (A) gelling properties of F3b (B) gelling properties of F3c (C) gelling properties of F3d (D) gelling properties of F3e at (E) at room temperature (1) and (2) body temperature.

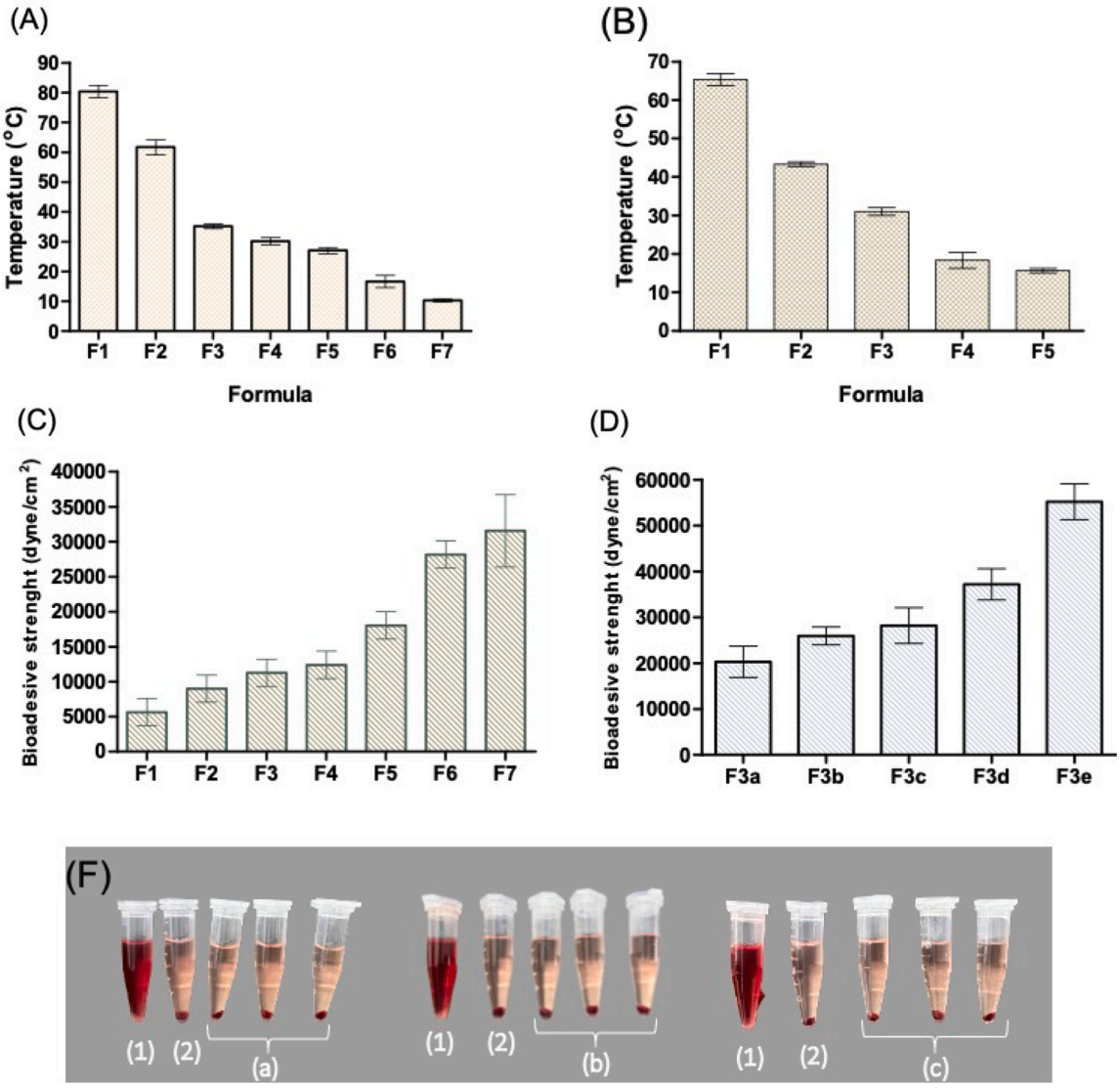

Fig. 6. Representation picture of gelation temperature for preliminary formula (A); affirmation test of gelling temperature after addition of 0.5 % HPMC (B); bioadhesive strength for Preliminary formulation (C); Bioadhesive strength for Optimized formulation (D) (means ± SD, n = 3). Visualize image of the hemolytic assay for CAP-MP's in thermoresponsive gel (all done in triplicates), group of 500 ppm; (a) 50 ppm; (b) 5 ppm; (c) positive (1) and negative control (2).

temperature. Notably, Pluronic® F127 and F68 have opposite effects on the gelation temperature. The inclusion of Pluronic® F68 into F127 was also observed by Khattab et al. to evaluate the formulation's gelation temperature (Khattab et al., 2019).

Pluronic® F127 gel preparations with higher Pluronic® F127 concentrations had lower Tsol-gel temperatures. Alternatively, as Pluronic® F68 concentration was raised, the gelation temperature rose. It is believed that the structural dissimilarity between Pluronic® F127 and F68 is to blame for this phenomenon. Pluronic® consists mostly of a central PPO block and two side PEO blocks. At a critical concentration and temperature, Pluronic undergoes gelation, which causes the hydrophobic PPO block to dehydrate while the hydrophilic PEO block was hydrated. Changing the PPO/PEO ratio affects the gelation temperature; adding a hydrophobic PPO block will decrease Tsol-gel whereas adding a hydrophilic PEO block increases it (Krtalić et al., 2018).

For further investigation, F1-F5 was chosen to see the effect of HPMC addition excluding those formulas that form a gel at room temperature (F6-F7). It was found that the addition of HPMC (0.5 %) as what shown in Fig. 6B did cause significant alteration in the Tsol-gel. The F1-F2 still could not reach the gelling temperature based on the physiological properties of the body, so the F3 was chosen to be used in the optimized formula. The optimized formula consists of a variety of HPMC concentrations classified into F3a, F3b, F3c, F3d, and F3e. This is to confirm how much HPMC concentration should be added to the formulation to achieve the best properties of gelling temperature. From the test, it was found that F3c showed the best temperature, based on physiological factors, and could still form a liquid at room temperature.

Because of the important role they've played in biological applications, sol–gel transformation in HPMC (hydroxypropyl methylcellulose) was receiving a growing amount of attention in research. The characteristics of HPMC and its concentration of it in the formula both have a significant impact on the thermo-reversible behavior of HPMC. Understanding the progression of the process of gelation within the context of the human body was aided by the findings of Joshi et al.'s experiments, which were conducted at or near the temperature of the human body. The comprehensive analysis of a variety of interactions at the molecular level unveiled the sol–gel mechanisms and the influence of a few other parameters. It was common knowledge that the hydrophobic groups of HPMC were exposed, intermolecular interaction occurs, and new connections were formed in the gel network. The sol–gel transformation occurred solely because of the hydrophobic interaction of HPMC chains, and the water cages mechanism was destroyed during heating (Joshi, 2011).

4.3.2. Bioadhesive strength evaluation

The length of time the preparation makes contact with the mucosal layer also has a significant role in determining the mucosal drug's bioavailability when it was applied topically. The effect of the polymer in preliminary formulas (F1-F7) was also investigated between Pluronic® F127 and F86 to determine mucoadhesive strength properties. The results of this study appear in Fig. 6C. The findings were compared to the optimized formula (F3a-F3e) after HPMC addition in various concentrations, and HPMC had a significant effect on the mucoadhesive properties of the gel formulations ($p < 0.05$) Fig. 6D. Furthermore, the thermoresponsive gel without a mucoadhesive agent showed the lowest mucoadhesive value compared to the optimized gel formulation. The results of the study on bio adhesion done by Notario et al. were encouraging. HPMC-only films successfully maintained adhesion to the tissue until they were completely eroded. This remained true up until the films were thoroughly cleansed. Hydrogen bonding in HPMC was responsible for its sticky properties. The same results being found in our formulation were an expected conclusion (Notario-Pérez et al., 2017, 2019). Consider also that Pluronic®, the main polymer in the thermoresponsive gel, has less mucoadhesive properties when compared to Carbopol, HPMC, and several other adhesive materials (Russo & Villa, 2019). In the absence of HPMC, the hydroxyl contacts between Pluronic® F127/F68 and the mucosal layer were not as strong as it was when the polymer was coupled with HPMC to form a thermoresponsive gel. Therefore, the mucoadhesive qualities of this combination were significantly improved. Researchers have found that HPMC, a cellulose derivative, has excellent mucoadhesive qualities (Chowhan & Giri, 2020). As the presentation of HPMC in the optimized formulation increased, so did the mucoadhesive strength, as shown by the optimization findings. Many studies, however, have demonstrated that Pluronic® F127 alone does not provide sufficient mucoadhesion (Kurniawansyah et al., 2020). Therefore, the incorporation of additional polymers, such as HPMC, is essential for elongating the period of time that the dosage form was presented on the surface of the skin. This will, as a result, contribute to an increase in the efficacy of preparations that were administered via the cutaneous route.

4.3.3. Viscosity study and rheological properties

At room temperature, in situ gel preparations take the form of a solution; nevertheless, they were able to become a gel substance when coming into contact with certain physiological circumstances. This is one of the most desirable characteristics of in situ gel preparations. When the preparation is being administered, having it in the form of a solution will help ensure that the dosage is accurate. As a result, it is essential to evaluate the difference in viscosity between the gel in situ preparation at the temperature of storage and the temperature that was physiologically appropriate for the skin. In this study, the viscosity of an optimized recipe for a thermoresponsive gel was measured in three different environments, classified into 4∘C as representative at cold temperature, 25∘C for room temperature, and 35∘C for body temperature. This is because thermoresponsive gels need to have gel characteristics at body temperature to improve localization time, but a free-flowing viscosity below body temperature to facilitate its application to the skin (Enggi et al., 2021). It is observed that the viscosities of five optimized thermoresponsive gel formulas in the body temperature were statistically ($p < 0.05$) different. The higher addition of polymer concentrations also increases the viscosity of the preparation. In a study conducted by Bercea et. al. with a temperature below 25 °C, the sample's viscoelastic moduli viscosity was significantly lower but slightly rose - beyond this temperature. This may be due to a rise in temperature-induced intermolecular interactions (Bercea et al., 2022). The low viscosity of the thermoresponsive formulations at cold and room temperatures was an essential indicator of their tendency towards the liquid form. Viscosity values lower than 30,000 mPa.s at body temperature were observed in all formulations, indicating the effective approach of our methods (Enggi et al., 2021). These findings were in keeping with the optimized formula's gelation temperature measurement, which showed that an increase in HPMC concentration led to gel formation at the desired temperatures. This reaffirms the benefits of combining Pluronic® F127 and F68 with the inclusion of HPMC for in situ gel formulations to achieve the desired viscosity during storage and application. All tested thermoresponsive gels in body temperature also demonstrate pseudoplastic performance. The rheological properties and viscosities were depicted in Fig. 7C and Fig. 7F, respectively.

4.3.4. pH measurement

Topical drug delivery systems were created for use in the skin's natural pH range (about 6) for optimal efficacy. For example, the drug's solubility in the formulation and the product's propensity to induce skin irritation can be affected by the formulation's pH. The shifting of the pH during the course of a product's shelf life could also point to a problem with stability (Anjali et al., n.d.). The pH values of the optimized formulations showed no significant difference ($p > 0.05$). Since all the formulations were in the pH range of 6, for this reason, all of the formulations' pH levels were already within the safe, healthy range for human skin, thus no further pH adjustment was necessary (Patel & Patel, 2012). Results showed optimal physicochemical properties of poloxamer 407 hydrogel which has a biocompatible pH value of 4.6 ± 0.1

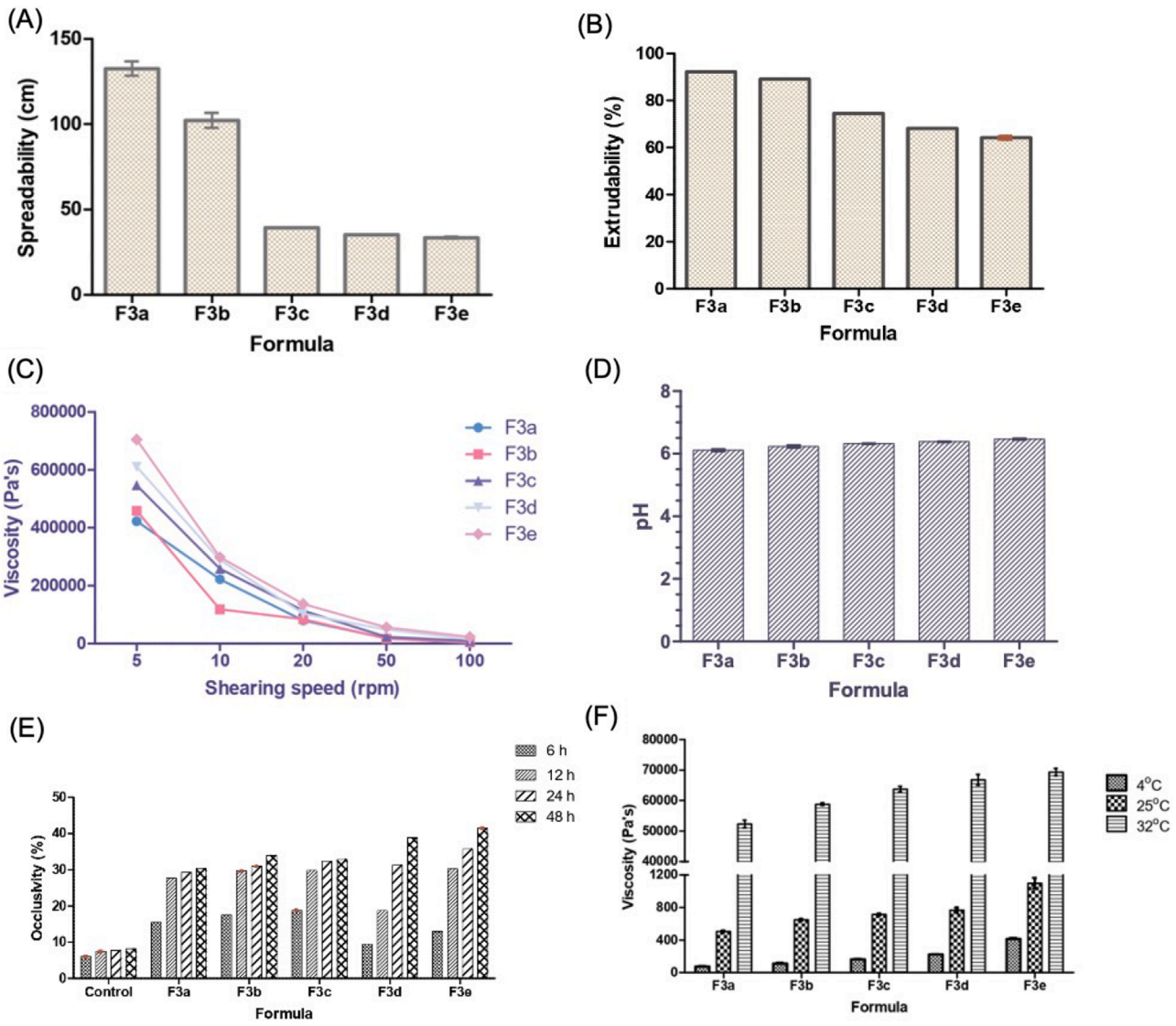

Fig. 7. Spreadability of optimized formulation (A); Extrudability of CAP-MP's in thermoresponsive gel (B), Rheological properties (C); pH (D); In vitro skin occlusivity in comparison with control (E), Viscosity in three different temperatures (F) (means ± SD, n = 3).

(Soriano-Ruiz et al., 2020).

4.3.5. Spreadability

Spreadability is a key indicator of how convenient a topical dosage form will be (Bercea et al., 2022). It is important that gels have adequate spreadability and meet the standards for optimal topical administration. The spreadability of the semi-solid formulation was measured in terms of the average diameter of the spread circle. The larger the diameter, the more spreadability will occur. This is because when the scatter diameter was larger, more of the surface area will be covered by the gel (Bercea et al., 2022). The results showed that spreadability was inversely proportional when measured in the physiological temperature of the body, considering that F3a and F3b both had a higher spreadability due to the properties of still being liquid when the measurement was conducted (Patel & Patel, 2012). Values of the spreadability indicated that the gel formulations were easily spreadable and showed optimal properties of spreadability.

4.3.6. Extrudability properties

Gel application and patient satisfaction were both impacted by how easily gel can be squeezed out of the tube. If the gel's consistency is too high, it won't extrude, while if it's too low, it will flow too quickly out of the tube. Therefore, less force would be needed to expel the gel from the container and get the desired dosage for administration. This quality also includes the gel's surface spreading capacity under a given shearing force (Soriano-Ruiz et al., 2020). All gel formulations were evaluated for extrudability and the findings were presented in Fig. 7B. The number of drugs extruded from the tube was calculated, as > 90 % extrudability: excellent, >80 % extrudability: good, and > 70 % extrudability: fair. From the findings, it is shown that formulations of F3a and F3b had good extrudability, but the formulations of F3c, F3d, and F3e had only fair extrudability.

4.3.7. In vitro skin Occlusive-Ability evaluation

Evaluation of the occlusivity of the skin was performed in vitro in order to make a prediction about the capability of the formulation to preserve the moisture trait of the skin (Malik & Kaur, 2018). Fig. 7E depicts the outcomes of the in vitro skin occlusivity test. It was discovered that the addition of HPMC at the greatest possible concentration during the period of observation was able to produce a substantial rise in the occlusivity values ($p < 0.05$). A greater occlusivity has the ability to boost the skin's hydration over a period of 48 h, which in turn makes it possible for the medicine to penetrate deeper layers of the skin by reducing the gaps between corneocytes. (Ammar et al., 2016).

Analyzed statistically, there was no significant difference ($p > 0.05$) in occlusivity values between the F3a, F3b, and F3c formulations.

4.3.8. In vitro hemolytic activity

In order to investigate the substance's initial toxicity of CAP-MP'S thermoresponsive gel against erythrocytes, a hemolytic activity test was performed on Wistar rats (Greco et al., 2020). The results obtained were shown in Fig. 6F. It was easy to observe that CAP-MP's in thermoresponsive gels had not shown any evidence of significant hemolysis values (<5%) in the concentrations that were tested in triplicates. This is something that can also be noticed in the serum or plasma which has become clearer and more transparent after being treated. Past literature states that the hemolysis index should be<5 % in order to meet the recommendations (Mir et al., 2020). As long as they fall within this range, the chemicals that were examined can be trusted. Therefore, based on the results obtained, it clearly indicated that CAP-MP's thermoresponsive gels were considered to be safe to use at the observed concentration.

4.3.9. Ex vivo dermatokinetic studies

The primary purpose of the transformation of CAP-MP's into a thermoresponsive in situ gel preparation was to boost the therapeutic efficacy of the treatment after it had been administered. That is why determining the dermatokinetic properties of this product was a necessity (Permana et al., 2021b). The wound-simulated fluid served as the experimental subject for the ex vivo dermatokinetic research of the thermoresponsive in situ gel. The experiments carried out allowed a comparison to be made between chloramphenicol conventional gel preparation and CAP-MP's in thermoresponsive gel formulation that was distributed in the thermoresponsive gel. The experiments served as a negative control. Overall, it was found that the thermoresponsive gel formulation was able to improve CAP absorption after cutaneous injection. This was the conclusion reached by the researchers.

In Table 7, we see that after receiving either the thermoresponsive gel of CAP-MP's or the control (CAP in gel), the peak concentration (Cmax) was observed at 30.3 mg and 4.7 mg, respectively. Both the thermoresponsive gel and the control took 6 h to achieve their highest concentration (Tmax), with the mean residence time (MRT) being at 58.8 and 62.6 h, respectively. These three findings show that CAP's dermatokinetic profile can be improved by reducing its particle size to that of microparticles and incorporating them into the thermoresponsive in situ gel formulation. It is true that the ability of the thermoresponsive gel to lengthen the amount of time a substance spends in contact with the skin may be at the root of this improvement. There was a statistically significant difference ($p < 0.05$) between the AUC of the drug evaluated in the optimized formulation and the control, with the former showing 439.7 mg·h and the latter showing 61.0 mgh; this suggests that the longer the contact time, the more drug compound was deposited into the skin.

4.3.10. Antibacterial activity in ex vivo infection model

To conclude, a bacterial activity study was performed on the skin of rats that had been infected with S. aureus in order to demonstrate that this preparation has the potential to be a therapeutic candidate for treating bacterial infections that occur in the skin. The antibacterial activity observations that were performed after 24 h demonstrated that the addition of CAP-MP'S into the thermoresponsive in situ gel increased the antibacterial activity. These observations were carried out after the gel had been in place for 24 h. The evidence for this can be seen in Fig. 8A. After 24 h of incubation, the reduction of bacterial growth was unaffected by the delivery of a blank gel (without CAP). At the same time, the application of thermoresponsive in situ gel containing CAP-MP's showed remarkable results, with a percentage eradication of 99.95 % within the bacterial population after just 24 h. The results of this investigation suggest that optimizing the formulation of a thermoresponsive in situ gel that incorporates CAP-MP's may improve the drug's transport and localization in the skin, resulting in increased antibacterial activity. We created three distinct gels for this investigation. Improved delivery profiles were observed after a mucoadhesive compound was added to thermoresponsive gels to boost their bioadhesiveness. In addition, the formulation was in a liquid form that would dry into a gel once applied to the skin, making it easy to administer and meeting a key requirement for patient satisfaction.

Additionally, the improved dermatokinetic profile and increased antibacterial activity of the medication were due to the combination of whey protein as a carrier for CAP microparticles and a thermoresponsive gel system. Unlike the standard therapy for skin infections caused by Staphylococcus aureus, which uses the same antimicrobial agent but was taken orally, this unique product clearly contains distinct characteristics that will aid in the development of treatment for these infections. This work highlights the need for additional in vivo research on the pharmacokinetic characteristics of CAP-MP's following topical application. It was crucial to compare the CAP-MP's pharmacokinetic profiles using this method to those obtained via injection or oral administration, the two primary modes of administration currently in use. Furthermore, human acceptability and usability testing was required before any clinical implementation.

5. Conclusion

The experimental findings show that the formulation of CAP into microparticles (MP's) administered via a thermoresponsive in situ gel system was superior to conventional CAP use. The drug's solubility was improved, and its residence time in the skin was lengthened by incorporating CAP into the MP's. This proves that this preparation can be a good candidate for the treatment of bacterial infection caused by Staphylococcus aureus. Moving forward, in vivo studies with a suitable animal model were highly recommended to investigate the pharmacokinetics profiles and to test the efficacy of this therapy in greater depth in an effort to develop better treatments for Staphylococcus aureus in skin bacterial infection.

CRediT authorship contribution statement

Ardiyah Nurul Fitri Marzaman: Conceptualization, Methodology, Visualization, Investigation, Formal analysis, Data curation, Writing – original draft, Writing – review & editing. **Sartini:** Conceptualization, Supervision, Writing – review & editing. **Mukarram Mudjahid:** Methodology, Investigation, Writing – review & editing. **Tri Puspita Roska:** Methodology, Resources, Writing – review & editing. **Anwar Sam:** Visualization. **Andi Dian Permana:** Investigation, Conceptualization, Resources, Writing – review & editing, Supervision, Funding acquisition.

Table 7
Dermatokinetics parameter of CAP-MP's in wound simulated fluid on infected rat skin (means ± SD, n = 3).

Media	Formulation	Cmax (μg/ml)	Tmax (h)	T ½ (h)	AUC (μg/ml*h)	MRT (h)
Wound Simulated Fluid	CAP-only in conventional Gel	4.78 ± 0.42	6 ± 0.8	40.55 ± 17.48	61.00 ± 5.56	62.68 ± 24.85
	CAP-MP's in Thermoresponsive gel	30.3 ± 1.66	6 ± 0	39.2 ± 18.5	439.7 ± 35.72	58.83 ± 26.55

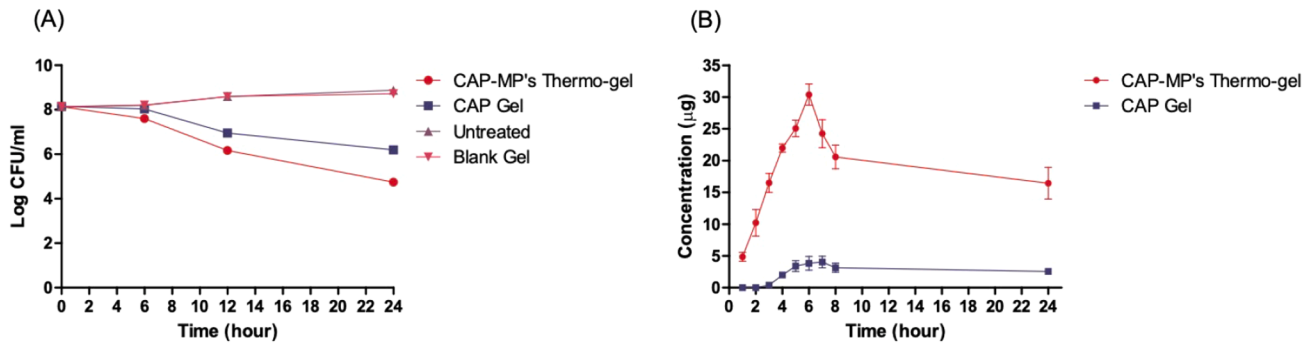

Fig. 8. Antibacterial activity of the ex vivo infection model (A); Dermatokinetic studies of CAP-MP's in thermoresponsive gel and CAP in conventional gel (B) (means ± SD, n = 3).

Declaration of Competing Interest

The authors declare that they have no known competing financial interests or personal relationships that could have appeared to influence the work reported in this paper.

Data availability

No data was used for the research described in the article.

Acknowledgment

Ardiyah Nurul Fitri Marzaman is very thankful to the German Academic Exchange Service (DAAD) which has given her the opportunity to gain more knowledge at Hasanuddin University by giving her a scholarship for a master's degree in pharmaceutical science (Ref. no. 91817973). The research project was also supported by the Ministry of Education, Culture, Research, and Technology of Indonesia by granting "Penelitian Tesis Magister" (090/E5/PG.02.00/PT/2022).

The authors also acknowledge the generosity of Glanbia Nutritionals, Inc, Fitchburg, USA and BASF SE (Jakarta, Indonesia) for providing whey protein isolate (WPI) and Pluronic® F68, respectively.

References

Aiyalu, R., Govindarjan, A., Ramasamy, A., 2016. Formulation and evaluation of topical herbal gel for the treatment of arthritis in animal model. Brazilian Journal of Pharmaceutical Sciences 52, 493–507. https://doi.org/10.1590/s1984-82502016000300015.

Alshirifi, A.N., Alhameedi, D.Y., n.d. New Spectrophotometric Determination of Chloramphenicol in Pharmaceutical Preparations Based on Condensation Reaction with 1,2-Naphthoquinone-4-Sulfonic Acid (1,2 NQS) as Reagent.

Ammar, H.O., Ghorab, M.M., Mostafa, D.M., Ibrahim, E.S., 2016. Folic acid loaded lipid nanocarriers with promoted skin antiaging and antioxidant efficacy. J Drug Deliv Sci Technol 31, 72–82. https://doi.org/10.1016/j.jddst.2015.11.007.

Anjali, C.H., Dash, M., Chandrasekaran, N., Mukherjee, A., n.d. ANTI BACTERIAL ACTIVITY OF SUNFLOWER OIL MICROEMULSION.

Arafat, M., Sarfraz, M., AbuRuz, S., 2021. Development and In Vitro Evaluation of Controlled Release Viagra® Containing Poloxamer-188 Using Gastroplus™ PBPK Modeling Software for In Vivo Predictions and Pharmacokinetic Assessments. Pharmaceuticals (Basel) 14. https://doi.org/10.3390/ph14050479.

Bagheri, L., Madadlou, A., Yarmand, M., Mousavi, M.E., 2013. Nanoencapsulation of date palm pit extract in whey protein particles generated via desolvation method. Food Res. Int. 51, 866–871. https://doi.org/10.1016/j.foodres.2013.01.058.

Bercea, M., Constantin, M., Plugariu, I.A., Oana Daraba, M., Luminita Ichim, D., 2022. Thermosensitive gels of pullulan and poloxamer 407 as potential injectable biomaterials. J Mol Liq 362. https://doi.org/10.1016/j.molliq.2022.119717.

Botrel, D.A., Rodrigues, I.C.B., de Souza, H.J.B., de Fernandes, R.V., B.,, 2016. Application of inulin in thin-layer drying process of araticum (Annona crassiflora) pulp. LWT - Food Science and Technology 69, 32–39. https://doi.org/10.1016/j.lwt.2016.01.018.

Bourgeois, C., Gomaa, A.I., Lefèvre, T., Cansell, M., Subirade, M., 2019. Interaction of oil bodies proteins with phospholipid bilayers: A molecular level elucidation as revealed by infrared spectroscopy. Int J Biol Macromol 122, 873–881. https://doi.org/10.1016/j.ijbiomac.2018.10.211.

Cheung, K., Das, D.B., 2016. Microneedles for drug delivery: trends and progress. Drug Deliv 23, 2338–2354. https://doi.org/10.3109/10717544.2014.986309.

Chowhan, A., Giri, T.K., 2020. Polysaccharide as renewable responsive biopolymer for in situ gel in the delivery of drug through ocular route. Int J Biol Macromol 150, 559–572. https://doi.org/10.1016/j.ijbiomac.2020.02.097.

Clinton, A., Carter, T., 2015. Chronic wound biofilms: Pathogenesis and potential therapies. Lab Medicine 46, 277–284. https://doi.org/10.1309/LMBNSWKUI4JPN7SO.

Combrinck, J., Otto, A., du Plessis, J., 2014. Whey protein/polysaccharide-stabilized emulsions: Effect of polymer type and pH on release and topical delivery of salicylic acid. AAPS PharmSciTech 15, 588–600. https://doi.org/10.1208/s12249-014-0081-3.

Dahlman, D., Håkansson, A., Kral, A.H., Wenger, L., Ball, E.L., Novak, S.P., 2017. Behavioral characteristics and injection practices associated with skin and soft tissue infections among people who inject drugs: A community-based observational study. Subst Abus 38, 105–112. https://doi.org/10.1080/08897077.2016.1263592.

Dai, Lei, et al., 2016. The interaction between Zein and Lecithin in ethanol-water solution and characterization of Zein–Lecithin composite colloidal nanoparticles. PLoS One. https://doi.org/10.1371/journal.pone.0167172.

Enggi, C.K., Isa, H.T., Sulistiawati, S., Ardika, K.A.R., Wijaya, S., Asri, R.M., Mardikasari, S.A., Donnelly, R.F., Permana, A.D., 2021. Development of thermosensitive and mucoadhesive gels of cabotegravir for enhanced permeation and retention profiles in vaginal tissue: A proof of concept study. Int J Pharm 609. https://doi.org/10.1016/j.ijpharm.2021.121182.

Ferreira, I.S., Bettencourt, A.F., Gonçalves, L.M.D., Kasper, S., Bétrisey, B., Kikhney, J., Moter, A., Trampuz, A., Almeida, A.J., 2015. Activity of daptomycin- and vancomycin-loaded poly-epsilon-caprolactone microparticles against mature staphylococcal biofilms. Int J Nanomedicine 10, 4351–4366. https://doi.org/10.2147/IJN.S84108.

Goyal, A., Sharma, V., Sihag, M.K., Tomar, S.K., Arora, S., Sabikhi, L., Singh, A.K., 2015. Development and physico-chemical characterization of microencapsulated flaxseed oil powder: A functional ingredient for omega-3 fortification. Powder Technol 286, 527–537. https://doi.org/10.1016/j.powtec.2015.08.050.

Greco, I., Molchanova, N., Holmedal, E., Jenssen, H., Hummel, B.D., Watts, J.L., Håkansson, J., Hansen, P.R., Svenson, J., 2020. Correlation between hemolytic activity, cytotoxicity and systemic in vivo toxicity of synthetic antimicrobial peptides. Sci Rep 10, 13206. https://doi.org/10.1038/s41598-020-69995-9.

Hasan, N., Cao, J., Lee, J., Hlaing, S.P., Oshi, M.A., Naeem, M., Ki, M.H., Lee, B.L., Jung, Y., Yoo, J.W., 2019. Bacteria-targeted clindamycin loaded polymeric nanoparticles: Effect of surface charge on nanoparticle adhesion to MRSA, antibacterial activity, and wound healing. Pharmaceutics 11. https://doi.org/10.3390/pharmaceutics11050236.

Hasni, Imed, et al., 2011. Binding of cationic lipids to milk β-lactoglobulin. J Phys Chem B 115(20), 6683–6690. https://doi.org/10.1021/jp200045h.

Jia, ZhenBao, et al., 2016. Effect of covalent modification by (−)-epigallocatechin-3-gallate on physicochemical and functional properties of whey protein isolate. LWT - Food Sci Technol 66, 305–310. https://doi.org/10.1016/j.lwt.2015.10.054.

Joshi, S.C., 2011. Sol-Gel Behavior of Hydroxypropyl Methylcellulose (HPMC) in Ionic Media Including Drug Release. Materials 4, 1861–1905. https://doi.org/10.3390/ma4101861.

Kalita, S., Devi, B., Kandimalla, R., Sharma, K.K., Sharma, A., Kalita, K., Kataki, A.C., Kotoky, J., 2015. Chloramphenicol encapsulated in poly-ε-caprolactone-pluronic composite: Nanoparticles for treatment of MRSA-infected burn wounds. Int J Nanomedicine 10, 2971–2984. https://doi.org/10.2147/IJN.S75023.

Khan, A., Wang, C., Sun, X., Killpartrick, A., Guo, M., 2019. Physicochemical and Microstructural Properties of Polymerized Whey Protein Encapsulated 3,3′-Diindolylmethane Nanoparticles. Molecules 24, 702. https://doi.org/10.3390/molecules24040702.

Khattab, A., Marzok, S., Ibrahim, M., 2019. Development of optimized mucoadhesive thermosensitive pluronic based in situ gel for controlled delivery of Latanoprost: Antiglaucoma efficacy and stability approaches. J Drug Deliv Sci Technol 53, 101134. https://doi.org/10.1016/j.jddst.2019.101134.

Krtalić, I., Radošević, S., Hafner, A., Grassi, M., Nenadić, M., Cetina-Čižmek, B., Filipović-Grčić, J., Pepić, I., Lovrić, J., 2018. D-Optimal Design in the Development of Rheologically Improved In Situ Forming Ophthalmic Gel. J Pharm Sci 107, 1562–1571. https://doi.org/10.1016/j.xphs.2018.01.019.

Kurniawansyah, I.S., Rusdiana, T., Sopyan, I., Ramoko, H., Wahab, H.A., Subarnas, A., 2020. In situ ophthalmic gel forming systems of poloxamer 407 and hydroxypropyl methyl cellulose mixtures for sustained ocular delivery of chloramphenicole: optimization study by factorial design. Heliyon 6, e05365.

Lademann, J., Schaefer, H., Otberg, N., Teichmann, A., Blume-Peytavi, U., Sterry, W., 2004. Penetration von Mikropartikeln in die menschliche Haut. Der Hautarzt 55, 1117–1119. https://doi.org/10.1007/s00105-004-0841-1.

Lai, L.F., Guo, H.X., 2011. Preparation of new 5-fluorouracil-loaded zein nanoparticles for liver targeting. Int J Pharm 404, 317–323. https://doi.org/10.1016/j.ijpharm.2010.11.025.

Lee, Pei-En, Choo, Wee-Sim, 2015. Characterization of flaxseed oil emulsions. J Food Sci Technol 52(7), 4378—386. https://doi.org/10.1007/s13197-014-1495-3.

Luo, Y., Teng, Z., Wang, Q., 2012. Development of Zein Nanoparticles Coated with Carboxymethyl Chitosan for Encapsulation and Controlled Release of Vitamin D3. J Agric Food Chem 60, 836–843. https://doi.org/10.1021/jf204194z.

Majeed, A., Khan, N.A., 2019. Journal of Drug Delivery and Therapeutics Ocular in situ gel : An overview. Journal of Drug Delivery and Therapeutics 9, 337–347.

Malik, D.S., Kaur, G., 2018. Nanostructured gel for topical delivery of azelaic acid: Designing, characterization, and in-vitro evaluation. J Drug Deliv Sci Technol 47, 123–136. https://doi.org/10.1016/j.jddst.2018.07.008.

Mir, M., Ahmed, N., Permana, A.D., Rodgers, A.M., Donnelly, R.F., Rehman, A.U., 2019. Enhancement in site-specific delivery of carvacrol against methicillin resistant staphylococcus aureus induced skin infections using enzyme responsive nanoparticles: A proof of concept study. Pharmaceutics 11. https://doi.org/10.3390/pharmaceutics11110606.

Mir, M., Permana, A.D., Tekko, I.A., McCarthy, H.O., Ahmed, N., Rehman, Asim. ur., Donnelly, R.F., 2020. Microneedle liquid injection system assisted delivery of infection responsive nanoparticles: A promising approach for enhanced site-specific delivery of carvacrol against polymicrobial biofilms-infected wounds. Int J Pharm 587, 119643. 10.1016/j.ijpharm.2020.119643.

Niwa, T., Imagawa, Y., Yamazaki, H., 2015. Drug Interactions between Nine Antifungal Agents and Drugs Metabolized by Human Cytochromes P450. Curr Drug Metab 15, 651–679. https://doi.org/10.2174/1389200215666141125121511.

Notario-Pérez, F., Martín-Illana, A., Cazorla-Luna, R., Ruiz-Caro, R., Bedoya, L.-M., Tamayo, A., Rubio, J., Veiga, M.-D., 2017. Influence of Chitosan Swelling Behaviour on Controlled Release of Tenofovir from Mucoadhesive Vaginal Systems for Prevention of Sexual Transmission of HIV. Mar Drugs 15, 50. https://doi.org/10.3390/md15020050.

Notario-Pérez, F., Martín-Illana, A., Cazorla-Luna, R., Ruiz-Caro, R., Bedoya, L.-M., Peña, J., Veiga, M.-D., 2019. Development of mucoadhesive vaginal films based on HPMC and zein as novel formulations to prevent sexual transmission of HIV. Int J Pharm 570, 118643. https://doi.org/10.1016/j.ijpharm.2019.118643.

Ordoñez, M., Herrera, A., 2014. Morphologic and stability cassava starch matrices for encapsulating limonene by spray drying. Powder Technol 253, 89–97. https://doi.org/10.1016/j.powtec.2013.11.005.

Patel, A., Patel, J., 2012. Mucoadhesive Microemulsion Based Prolonged Release Vaginal Gel for Anti-Fungal Drug. Am. J. PharmTech Res 2.

Patel, A., Hu, Y., Tiwari, J.K., Velikov, K.P., 2010. Synthesis and characterisation of zein–curcumin colloidal particles. Soft Matter 6, 6192. https://doi.org/10.1039/c0sm00800a.

Permana, McCrudden, Donnelly, 2019. Enhanced Intradermal Delivery of Nanosuspensions of Antifilariasis Drugs Using Dissolving Microneedles: A Proof of Concept Study. Pharmaceutics 11, 346. 10.3390/pharmaceutics11070346.

Permana, A.D., Anjani, Q.K., Sartini, Utomo, E., Volpe-Zanutto, F., Paredes, A.J., Evary, Y.M., Mardikasari, S.A., Pratama, Muh.R., Tuany, I.N., Donnelly, R.F., 2021a. Selective delivery of silver nanoparticles for improved treatment of biofilm skin infection using bacteria-responsive microparticles loaded into dissolving microneedles. Materials Science and Engineering: C 120, 111786. 10.1016/j.msec.2020.111786.

Permana, A.D., Tekko, I.A., McCrudden, M.T.C., Anjani, Q.K., Ramadon, D., McCarthy, H.O., Donnelly, R.F., 2019. Solid lipid nanoparticle-based dissolving microneedles: A promising intradermal lymph targeting drug delivery system with potential for enhanced treatment of lymphatic filariasis. J. Control. Release 316, 34–52. https://doi.org/10.1016/j.jconrel.2019.10.004.

Permana, A.D., Mir, M., Utomo, E., Donnelly, R.F., 2020a. Bacterially sensitive nanoparticle-based dissolving microneedles of doxycycline for enhanced treatment of bacterial biofilm skin infection: A proof of concept study. Int J Pharm X 2, 100047. https://doi.org/10.1016/j.ijpx.2020.100047.

Permana, A.D., Utami, R.N., Courtenay, A.J., Manggau, M.A., Donnelly, R.F., Rahman, L., 2020b. Phytosomal nanocarriers as platforms for improved delivery of natural antioxidant and photoprotective compounds in propolis: An approach for enhanced both dissolution behaviour in biorelevant media and skin retention profiles. J Photochem Photobiol B 205. https://doi.org/10.1016/j.jphotobiol.2020.111846.

Permana, A.D., Utami, R.N., Layadi, P., Himawan, A., Juniarti, N., Anjani, Q.K., Utomo, E., Mardikasari, S.A., Arjuna, A., Donnelly, R.F., 2021. Thermosensitive and mucoadhesive in situ ocular gel for effective local delivery and antifungal activity of itraconazole nanocrystal in the treatment of fungal keratitis. Int J Pharm 602. https://doi.org/10.1016/j.ijpharm.2021.120623.

Picone, C.S.F., Takeuchi, K.P., Cunha, R.L., 2011. Heat-Induced Whey Protein Gels: Effects of pH and the Addition of Sodium Caseinate. Food Biophys 6, 77–83. https://doi.org/10.1007/s11483-010-9177-9.

Russo, E., Villa, C., 2019. Poloxamer Hydrogels for Biomedical Applications. Pharmaceutics 11, 671. https://doi.org/10.3390/pharmaceutics11120671.

Sağlam, D., Venema, P., de Vries, R., Sagis, L.M.C., van der Linden, E., 2011. Preparation of high protein micro-particles using two-step emulsification. Food Hydrocoll 25, 1139–1148. https://doi.org/10.1016/j.foodhyd.2010.10.011.

Sağlam, D., Venema, P., de Vries, R., Shi, J., van der Linden, E., 2013. Concentrated whey protein particle dispersions: Heat stability and rheological properties. Food Hydrocoll 30, 100–109. https://doi.org/10.1016/j.foodhyd.2012.05.005.

Sartini, S., Permana, A.D., Mitra, S., Tareq, A.M., Salim, E., Ahmad, I., Harapan, H., Emran, T. bin, Nainu, F., 2021. Current state and promising opportunities on pharmaceutical approaches in the treatment of polymicrobial diseases. Pathogens 10, 1–31. 10.3390/pathogens10020245.

Shahi, S., Thube, M., 2011. \376\377\000M\000I\000C\000R\000O\000P\000A\000R\000T\000I\000C\000L\000E\000S\000:\000 \000A\000N\000 \000A\000P\000P\000R\000O\000A\000C\000H\000 \000F\000O\000R\000 \000B\000E\000T\000T\000E\000R\000M\000E\000N\000T\000 \000O\000F\000 \000D\000R\000U\000G\000 \000D\000E\000L\000I\000V\000E\000R\000Y\000 \000S\000Y\000S\000T\000E\000M.

Sharma, N., Madan, P., Lin, S., 2016. Effect of process and formulation variables on the preparation of parenteral paclitaxel-loaded biodegradable polymeric nanoparticles: A co-surfactant study. Asian J Pharm Sci 11, 404–416. https://doi.org/10.1016/j.ajps.2015.09.004.

Shen, A.Y., Haddad, E.J., Hunter-Smith, D.J., Rozen, W.M., 2018a. Efficacy and adverse effects of topical chloramphenicol ointment use for surgical wounds: a systematic review. ANZ J Surg 88, 1243–1246. https://doi.org/10.1111/ans.14465.

Shen, X., Zhao, C., Lu, J., Guo, M., 2018b. Physicochemical Properties of Whey-Protein-Stabilized Astaxanthin Nanodispersion and Its Transport via a Caco-2 Monolayer. J Agric Food Chem 66, 1472–1478. https://doi.org/10.1021/acs.jafc.7b05284.

Silva Keven, Erik, et al., 2016. Ultrasound-assisted encapsulation of annatto seed oil: Whey protein isolate versus modified starch. Food Hydrocoll 56, 71–83. https://doi.org/10.1016/j.foodhyd.2015.12.006.

Silva, E.K., Meireles, M.A.A., 2015. Influence of the degree of inulin polymerization on the ultrasound-assisted encapsulation of annatto seed oil. Carbohydr Polym 133, 578–586. https://doi.org/10.1016/j.carbpol.2015.07.025.

Singhvi, G., Singh, M., n.d. International Journal of Pharmaceutical Studies and Research Review: In-Vitro Drug Release Characterization Models.

Soriano-Ruiz, J.L., Calpena-Campmany, A.C., Silva-Abreu, M., Halbout-Bellowa, L., Bozal-de Febrer, N., Rodríguez-Lagunas, M.J., Clares-Naveros, B., 2020. Design and evaluation of a multifunctional thermosensitive poloxamer-chitosan-hyaluronic acid gel for the treatment of skin burns. Int J Biol Macromol 142, 412–422. https://doi.org/10.1016/j.ijbiomac.2019.09.113.

Tadros, T., Izquierdo, P., Esquena, J., Solans, C., 2004. Formation and stability of nano-emulsions. Adv Colloid Interface Sci 108–109, 303–318. https://doi.org/10.1016/j.cis.2003.10.023.

Tang, D.-W., Yu, S.-H., Ho, Y.-C., Huang, B.-Q., Tsai, G.-J., Hsieh, H.-Y., Sung, H.-W., Mi, F.-L., 2013. Characterization of tea catechins-loaded nanoparticles prepared from chitosan and an edible polypeptide. Food Hydrocoll 30, 33–41. https://doi.org/10.1016/j.foodhyd.2012.04.014.

Teng, Z., Luo, Y., Wang, Q., 2013. Carboxymethyl chitosan-soy protein complex nanoparticles for the encapsulation and controlled release of vitamin D3. Food Chem 141, 524–532. https://doi.org/10.1016/j.foodchem.2013.03.043.

Wang, W., Hui, P.C.L., Ng, F.S.F., Kan, C.W., Lau, C.B.S., Leung, P.C., 2017. Application of thermosensitive poloxamer-based hydrogel in the development of transdermal therapy containing herbal medicine. Key Eng Mater 719, 57–61. https://doi.org/10.4028/www.scientific.net/KEM.719.57.

Wang, C., Zhou, X., Wang, H., Sun, X., Guo, M., 2019. Interactions between β-Lactoglobulin and 3,3′-Diindolylmethane in Model System. Molecules 24, 2151. https://doi.org/10.3390/molecules24112151.

Wu, J., Shi, M., Li, W., Zhao, L., Wang, Z., Yan, X., Norde, W., Li, Y., 2015. Pickering emulsions stabilized by whey protein nanoparticles prepared by thermal cross-linking. Colloids Surf B Biointerfaces 127, 96–104. https://doi.org/10.1016/j.colsurfb.2015.01.029.

Yi, Jiang, et al., 2015. Beta-carotene encapsulated in food protein nanoparticles reduces peroxyl radical oxidation in Caco-2 cells. Food Hydrocoll 43, 31–40. https://doi.org/10.1016/j.foodhyd.2014.04.028.

Zhang, Y., Huo, M., Zhou, J., Zou, A., Li, W., Yao, C., Xie, S., 2010. DDSolver: An Add-In Program for Modeling and Comparison of Drug Dissolution Profiles. AAPS J 12, 263–271. https://doi.org/10.1208/s12248-010-9185-1.